Photophysical Properties of Di-Schiff Bases: Evaluating the Synergistic Effect of Non Covalent Interactions and Alkyl Spacer in Enhanced Emissions in Solids

*Moyna Das, Fayaz Baig and Madhushree Sarkar**

Department of Chemistry, Birla Institute of Technology and Science, Pilani, Pilani Campus Rajasthan 333031, India; Email: msarkar@bits-pilani.ac.in Phone: +91-1596-515679; Fax: +91-1596-244183

SUPPORTING INFORMATION

General: Infra Red Spectra were taken in FTIR ABB Bomen MB-3000. UV-Visible Spectra and Fluorescence Spectra were taken in Shimadzu spectrophotometer with model UV-2450 and Fluorimax-4 0426C0809, respectively. Proton and Carbon-13 Nuclear Magnetic Resonance (^{1}H NMR and ^{13}C NMR) spectra were recorded on a 400 MHz spectrophotometer (Bruker). Powder X-Ray Diffraction (XRD) were recorded with a Rigaku miniflex ll, λ =1.54, Cu Kα.

Figure S1: IR of **L1a**

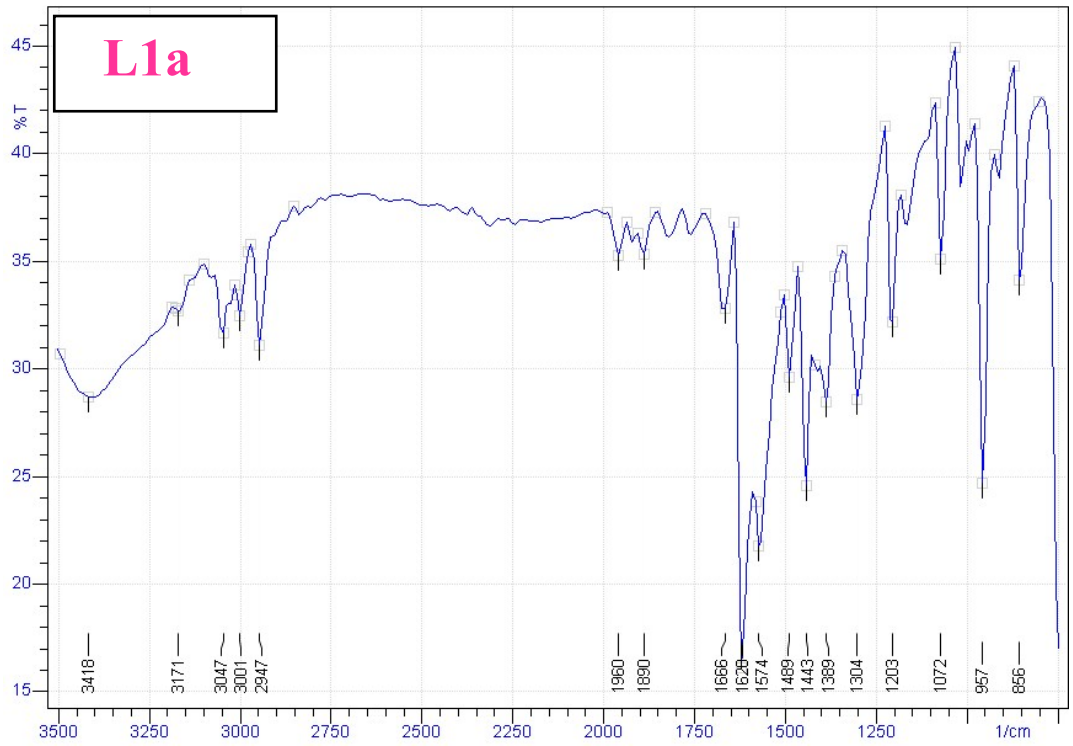

IR (cm^{-1} KBr pellet): 3418(w), 3171(w), 3047(w), 3001(w), 2947(m), 1666(m), 1628(vs), 1574(w), 489(w), 1443(m), 1304(w), 1203(w), 957(m), 856(w).

Figure S2: ^{1}H NMR of **L1a**

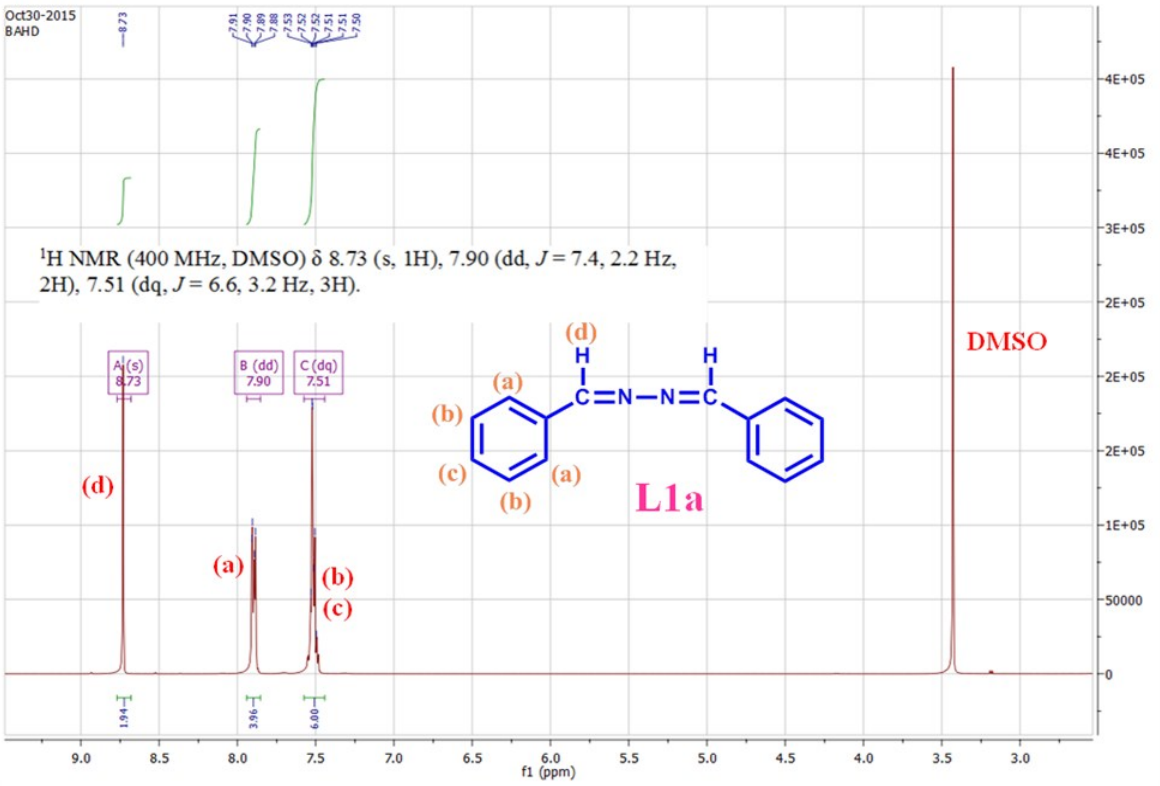

Figure S3: ^{13}C NMR of **L1a**

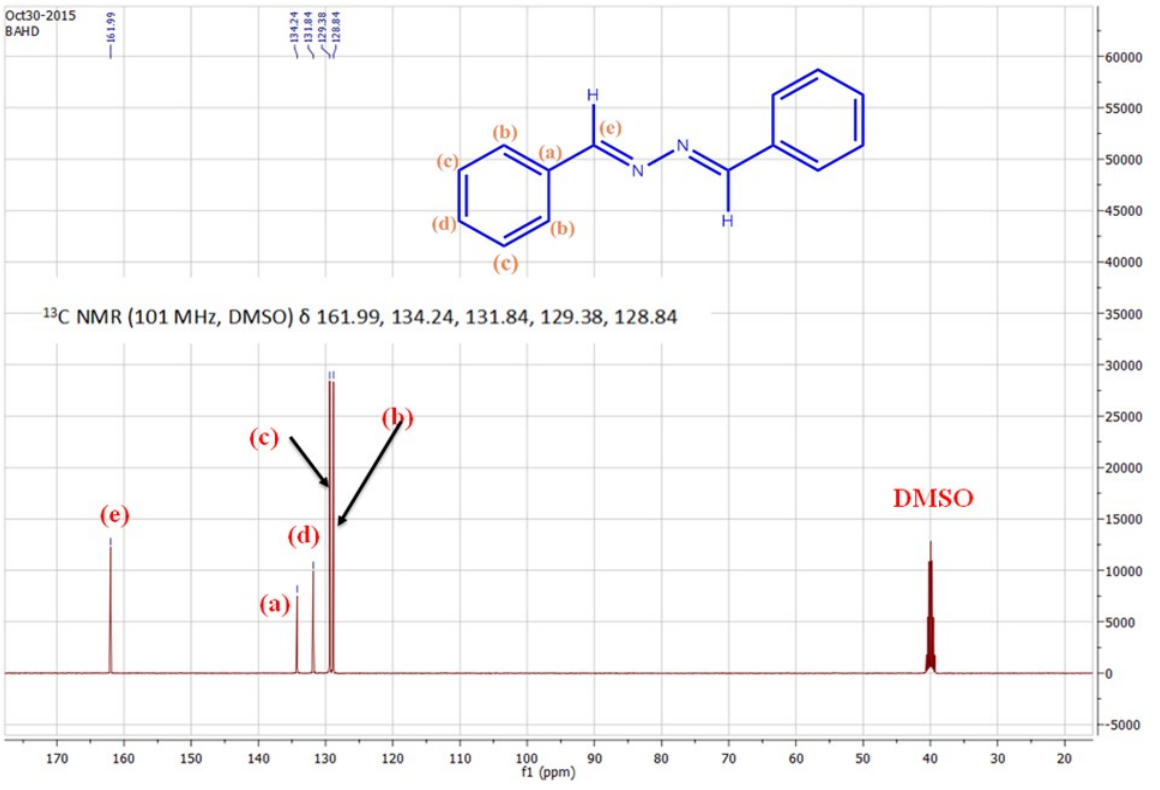

Figure S4: IR of **L1b**

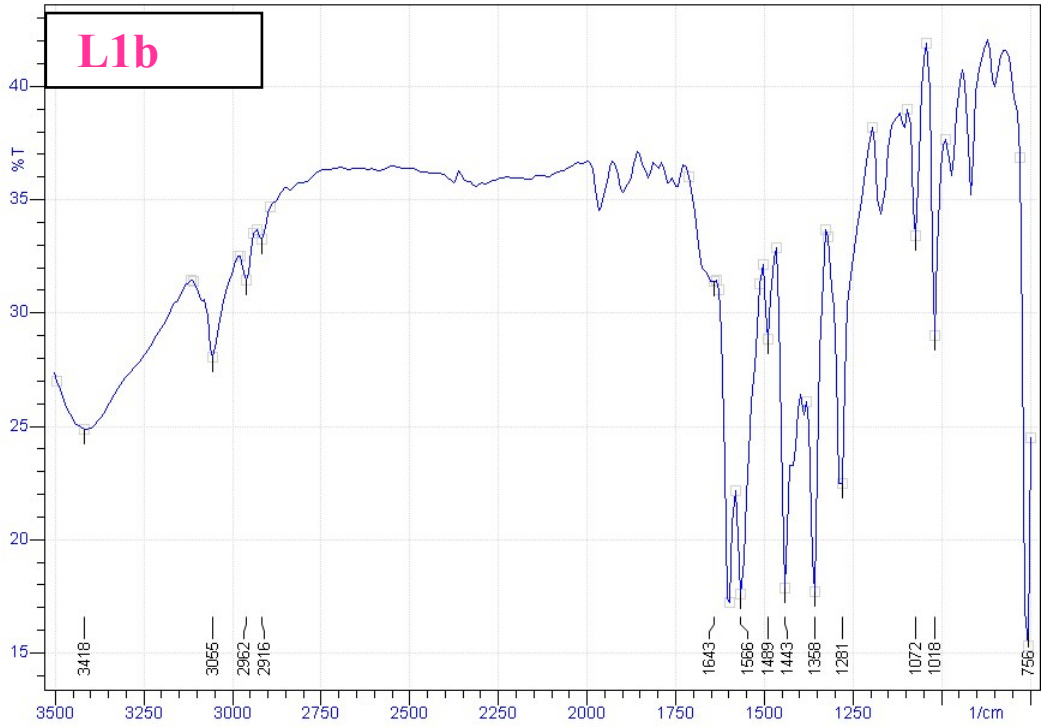

IR (cm^{-1} KBr pellet): 3418(m), 3055(m), 2962(m), 2916(w), 1643(vs), 1566(vs), 1489(w), 1443(vs), 1358(vs), 1281(s), 1072(m), 1018(m), 756(vs).

Figure S5: ^{1}H NMR of **L1b**

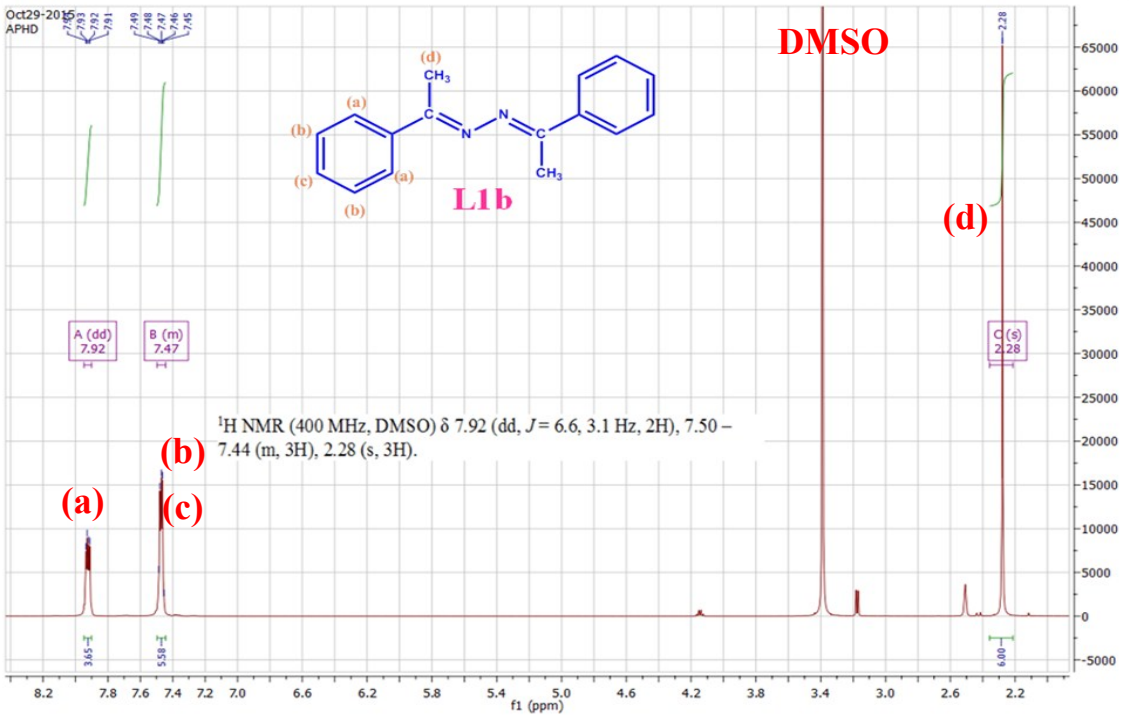

Figure S6: ^{13}C NMR of **L1b**

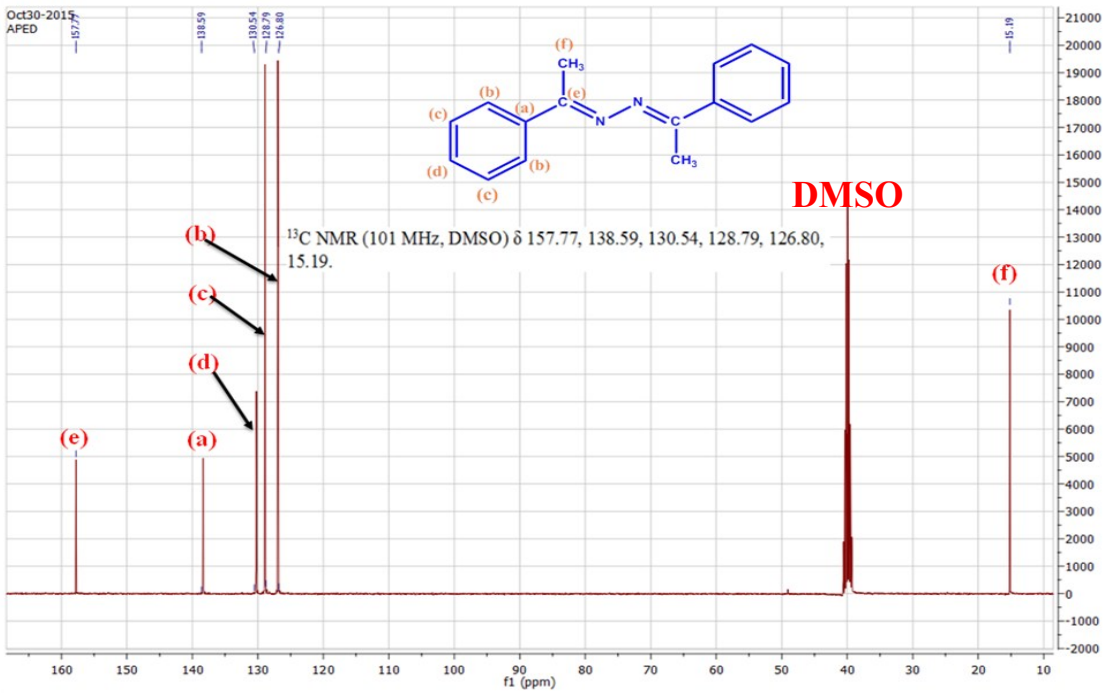

Figure S7: IR of **L2a**

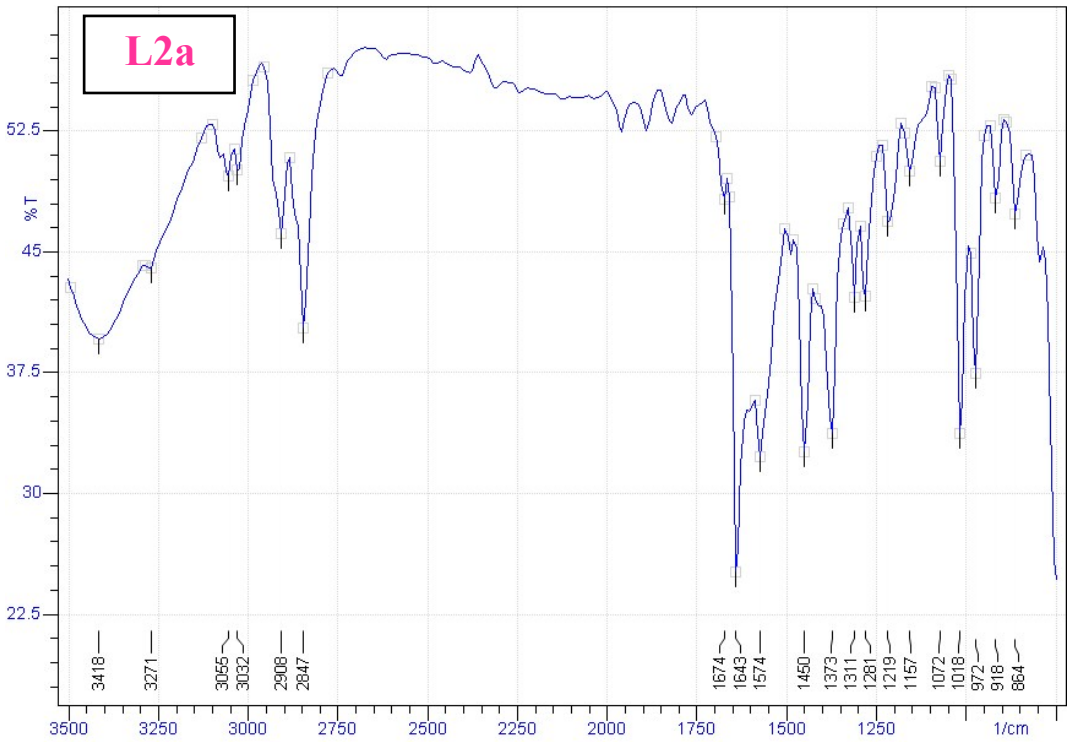

IR (cm^{-1} KBr pellet): 3418(m), 3271(w), 3055(w), 3032(w), 2908(w), 2843(m),1674(w), 1643(vs), 1574(w),1450(m), 1373(m), 1281(w), 157(w), 1018(s), 972(w), 918(w).

Figure S8: ^{1}H NMR of **L2a**

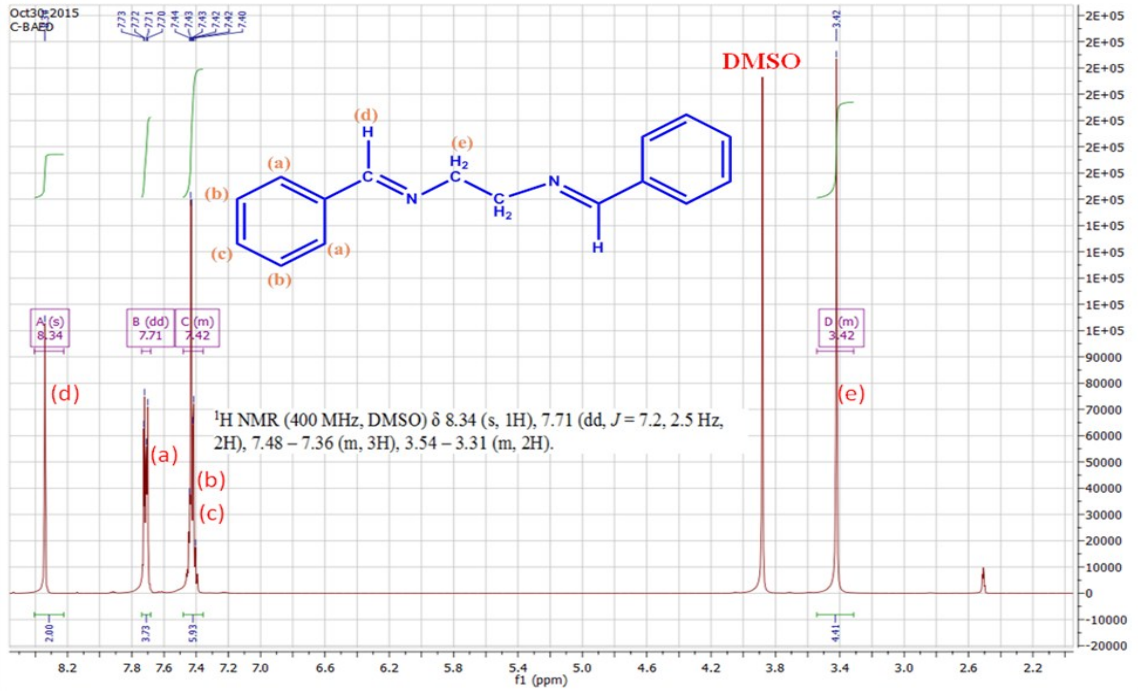

Figure S9: ^{13}C NMR of **L2a**

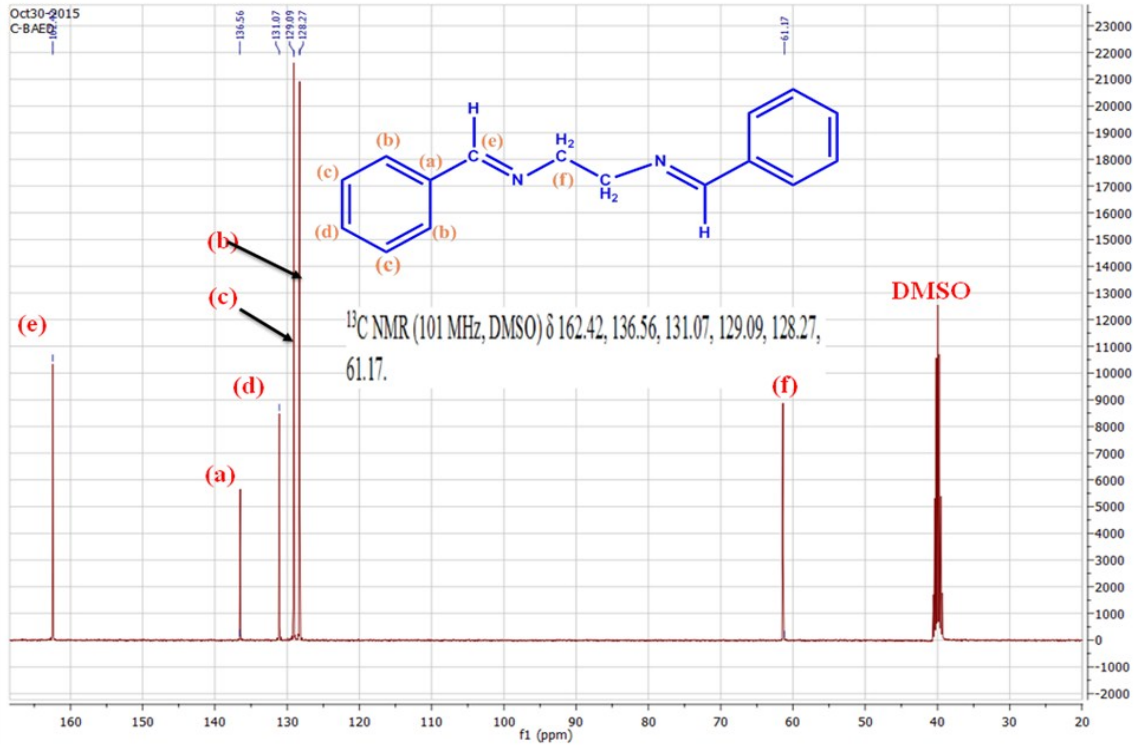

Figure S10: IR of **L2b**

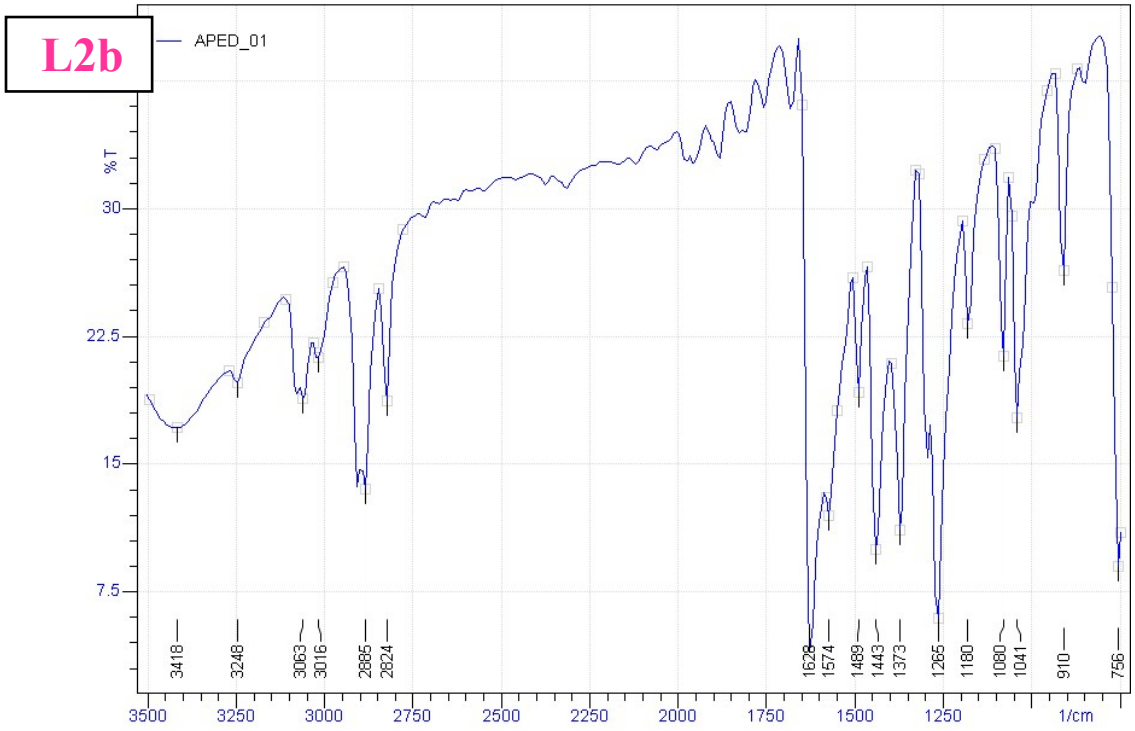

IR (cm^{-1} KBr pellet): 3418(m), 3248(w), 3063(w), 3016(w), 2885(m), 2824(m), 1628(vs), 1574(w), 1489(w), 1443(m), 1373(m), 1265(vs), 1180(w), 1080(m), 1041(m), 910(m),756(vs).

Figure S11: ^{1}H NMR of **L2b**

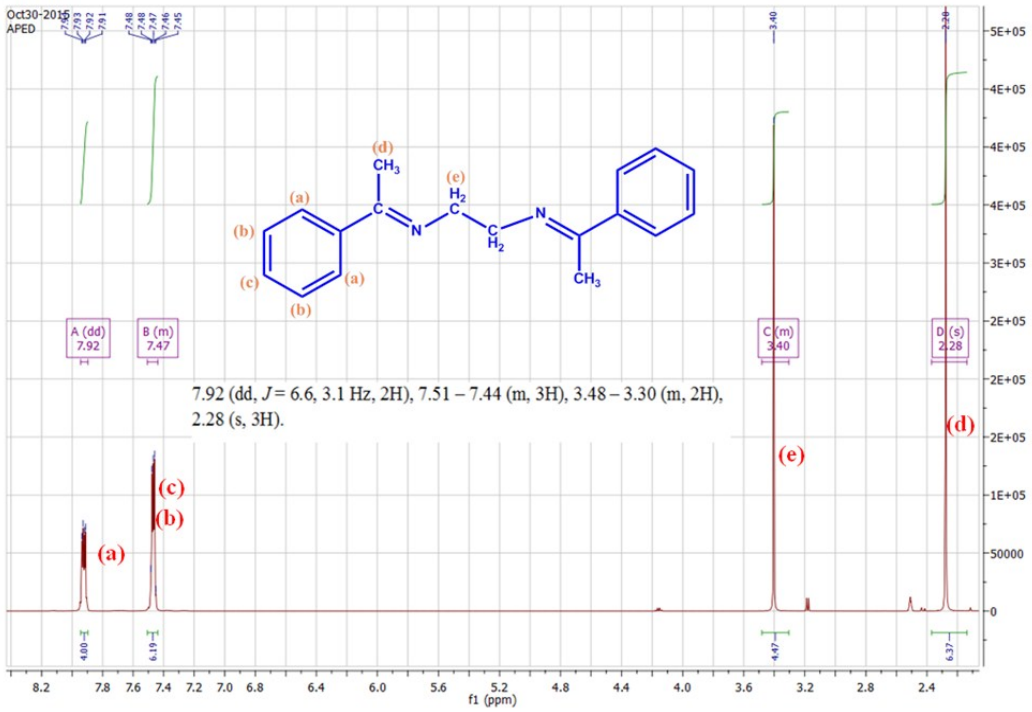

Figure S12: ^{13}C NMR of **L2b**

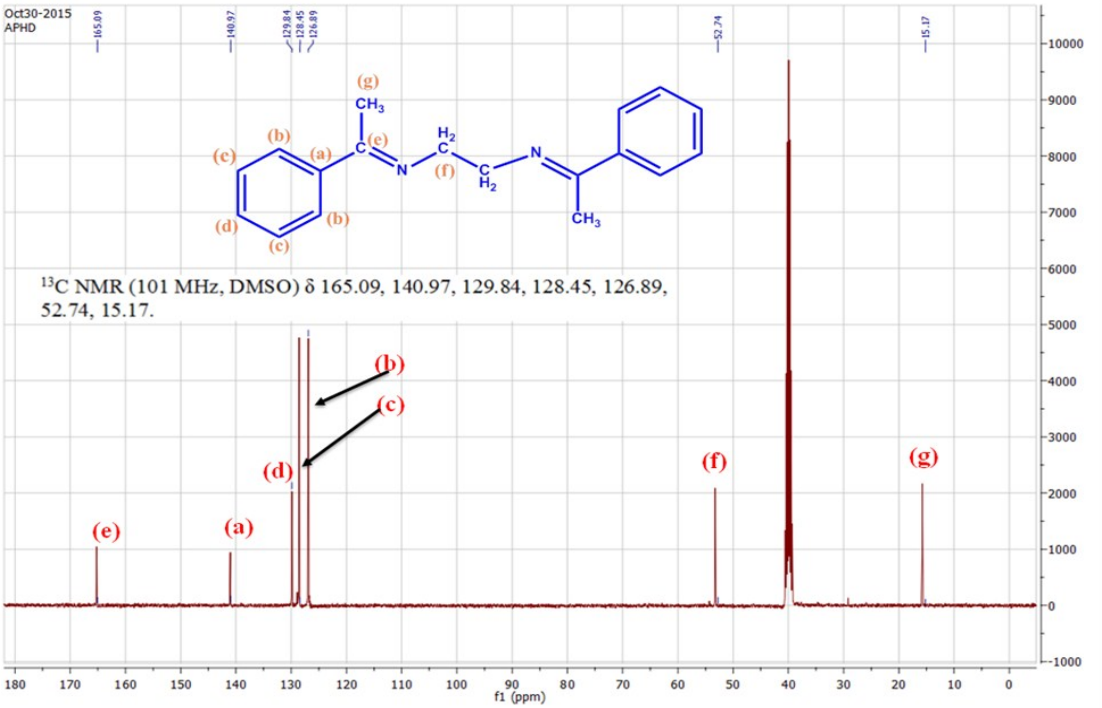

Figure S13: IR of **L3a**

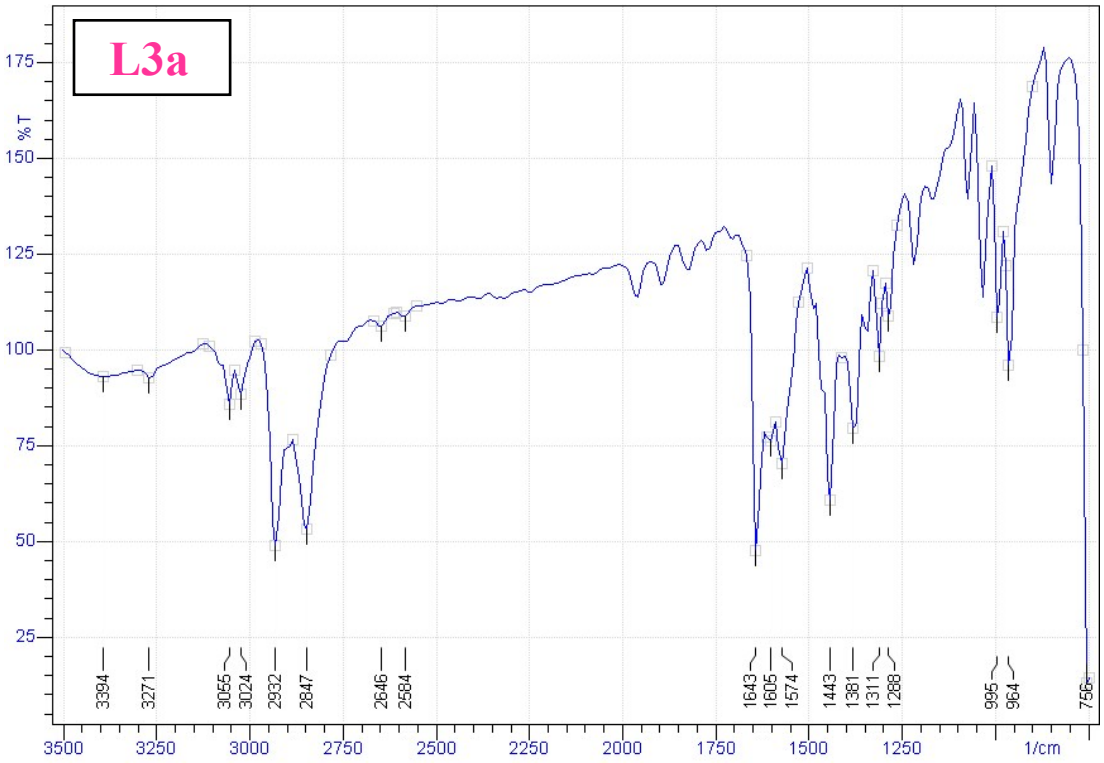

IR (cm^{-1} KBr pellet): 3394(w), 3271(w), 3055(w), 3024(w),2932(m), 2847(m),2646(w), 1643(vs), 1605(w), 1574(w), 1443(s), 1381(w), 1288(w), 965(w),756(vs).

Figure S14: ^{1}H NMR of **L3a**

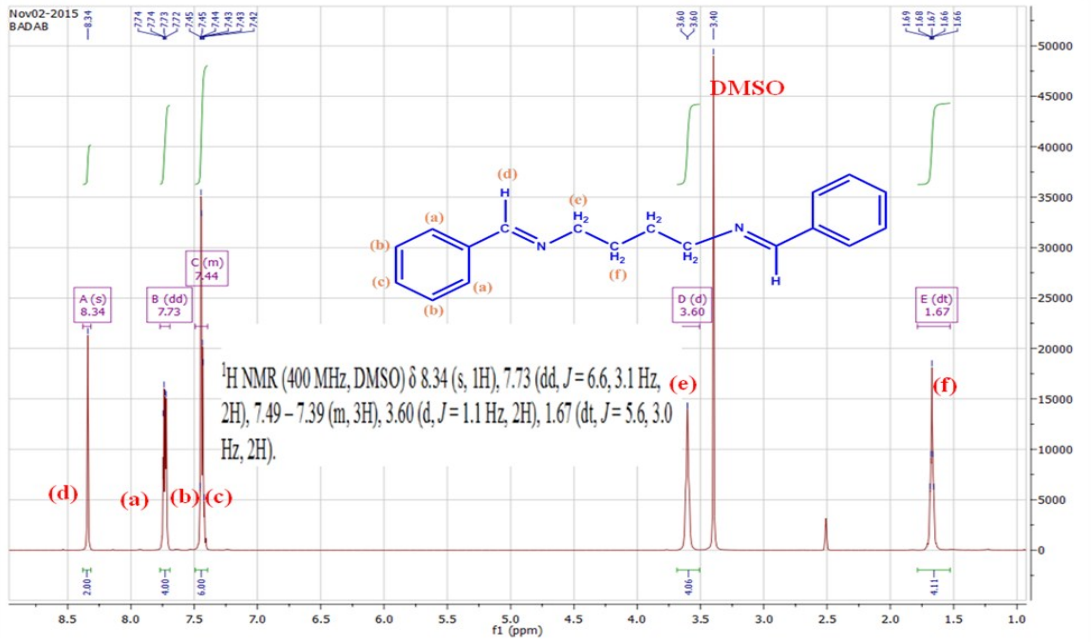

Figure S15: ^{13}C NMR of **L3a**

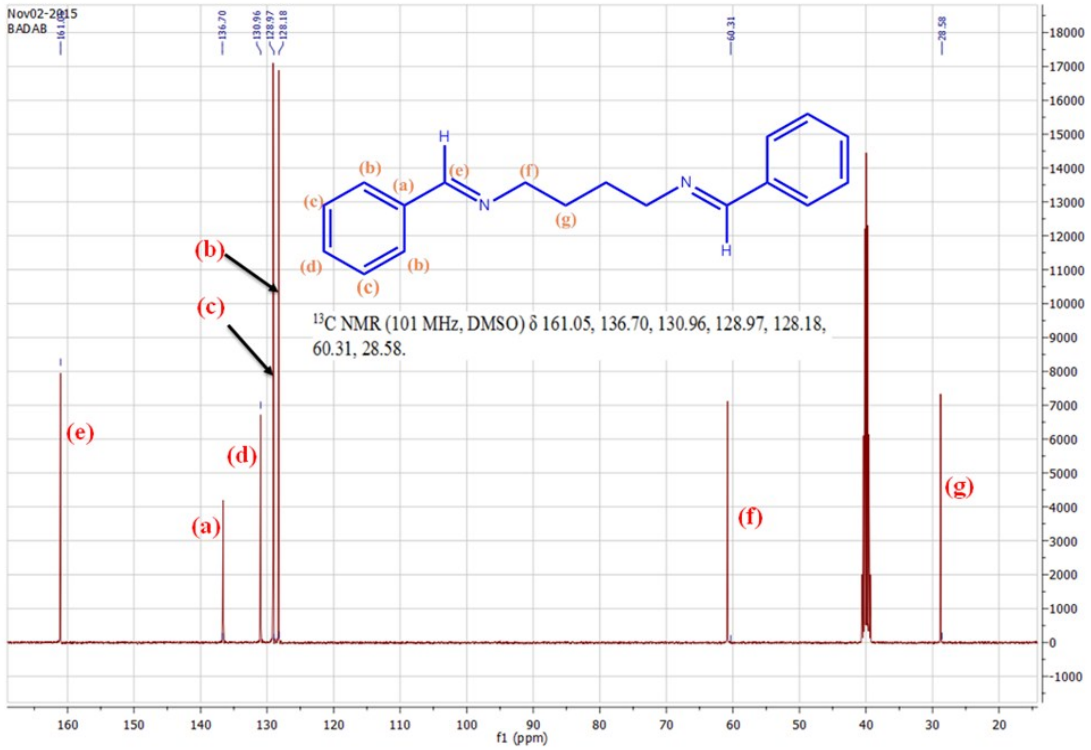

Figure S16: IR of **L3b**

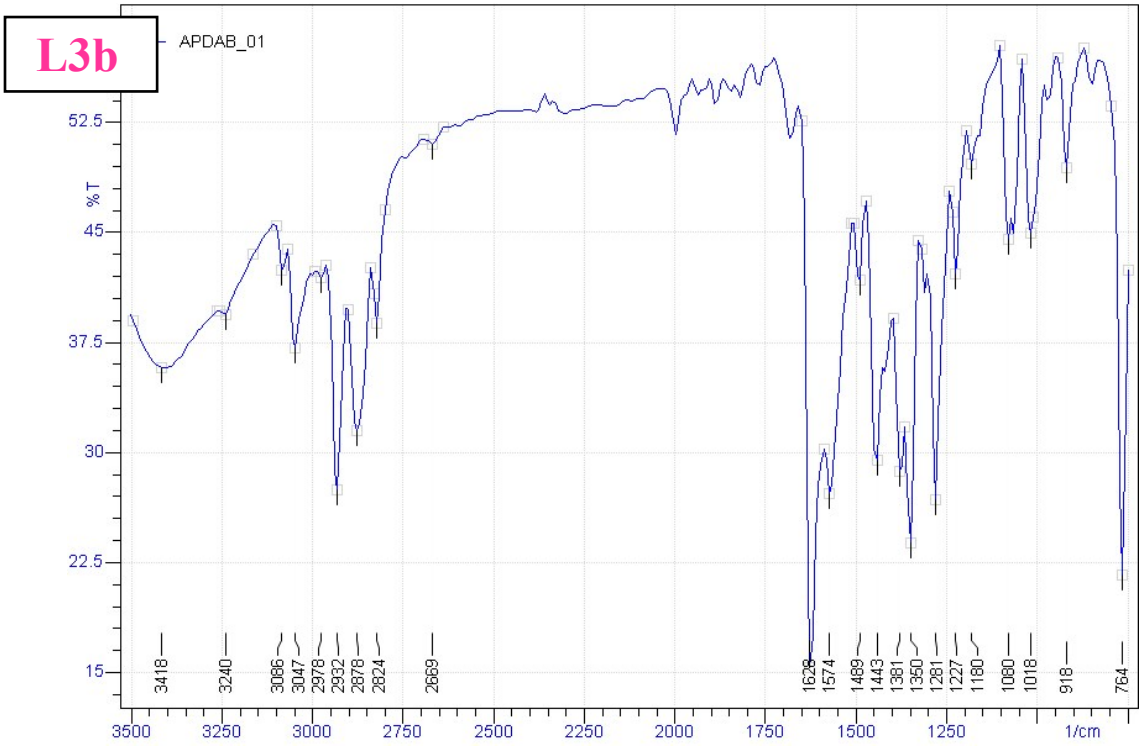

IR (cm^{-1} KBr pellet): 3418(m), 3240(w), 3086(w),3047(w), 2932(m), 2878(m), 1628(vs), 1574(w), 1489(w), 1443(w), 1350(m), 1281(m), 1180(w), 1080(w), 918(w),764(vs).

Figure S17: ^{1}H NMR of **L3b**

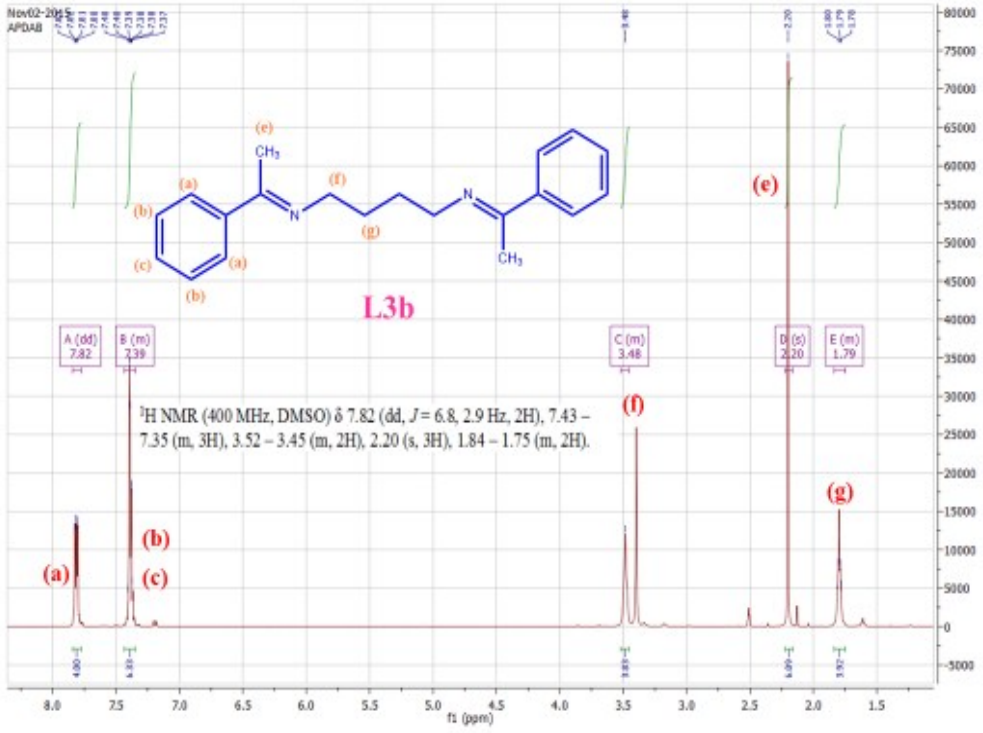

Figure S18: ^{13}C NMR of **L3b**

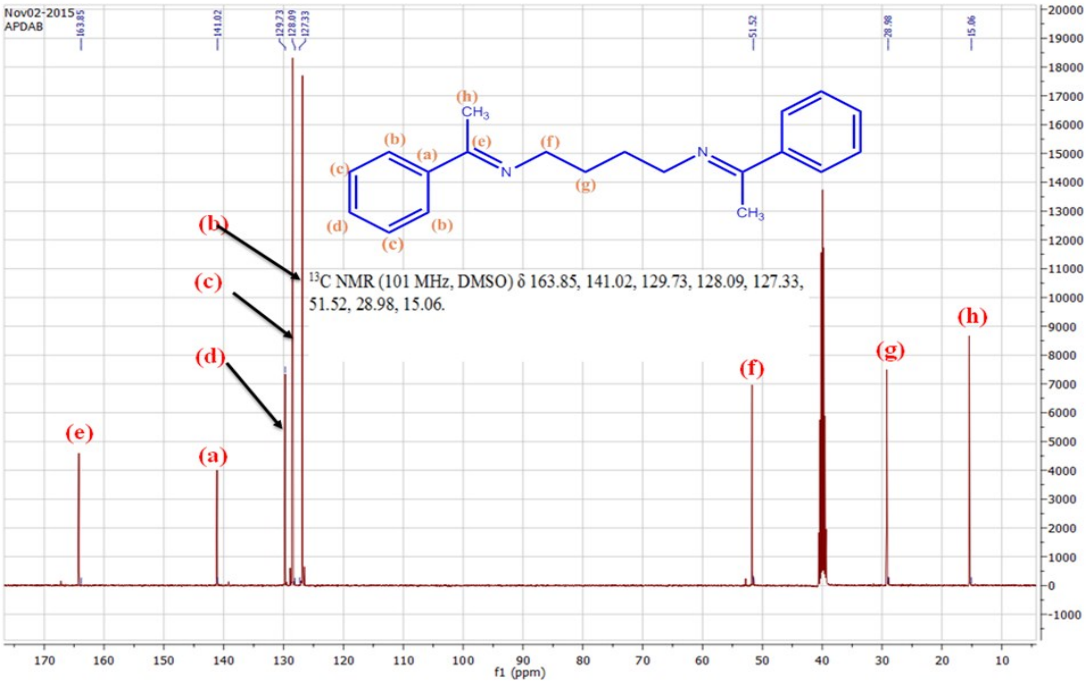

Figure S19: IR of **L4a**

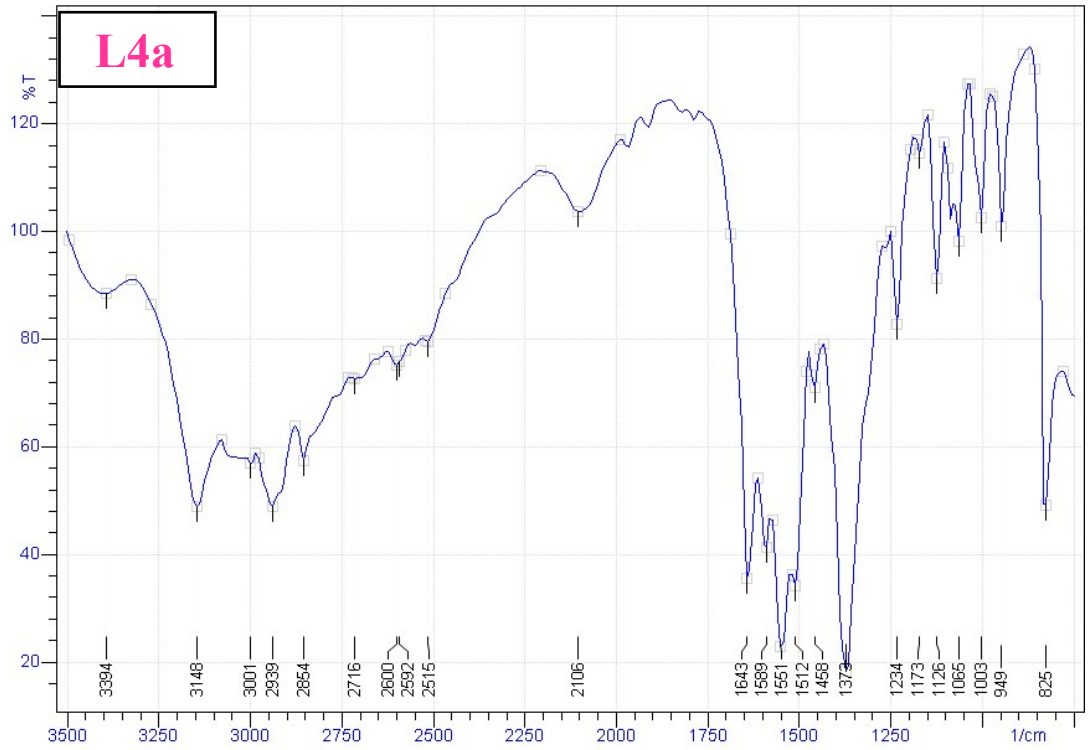

IR (cm^{-1} KBr pellet): 3394(w),3148(m), 3001(w), 2939(w), 2854(w), 2716(w), 2106(w), 1643(s), 1589(w), 1551(vs), 1379(vs), 1234(w), 1173(w), 1065(w), 949(w), 825(s).

Figure S20: ^{1}H NMR of **L4a**

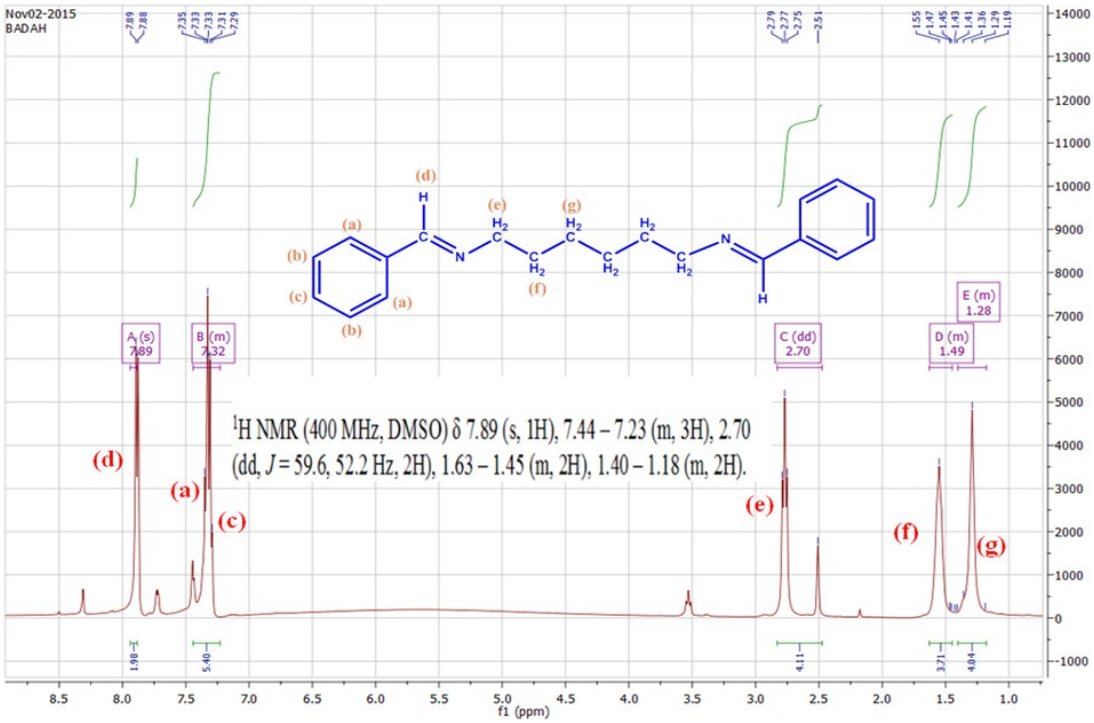

Figure S21: ^{13}C NMR of **L4a**

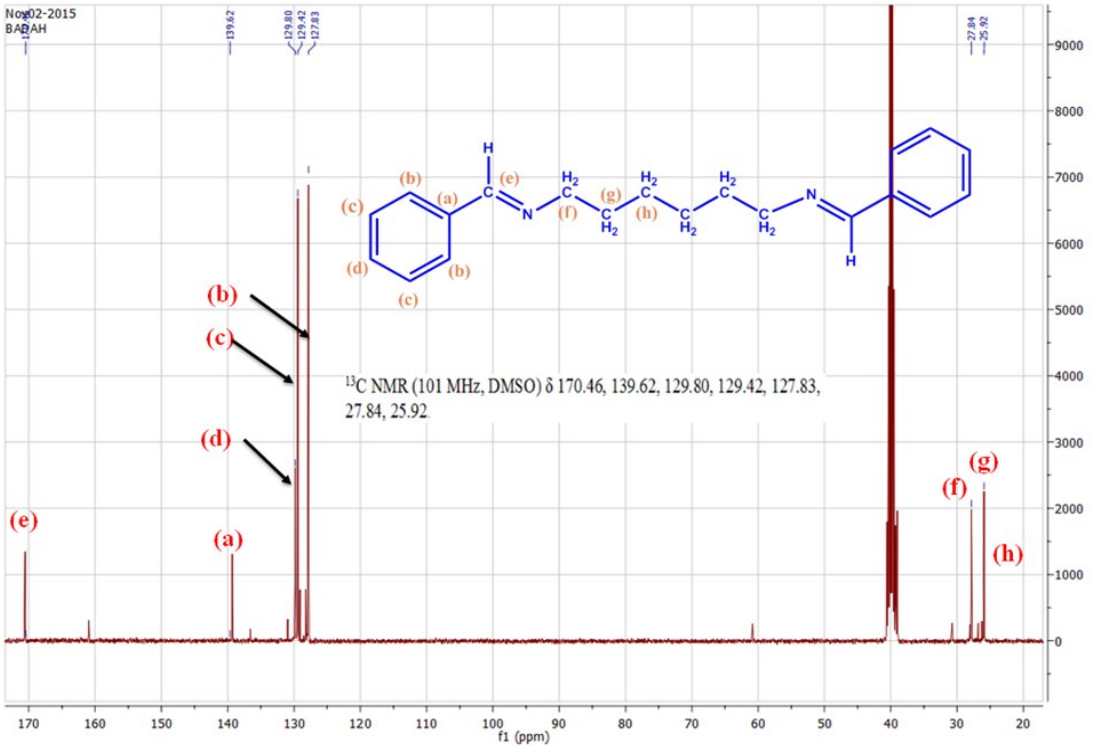

Figure S22: IR of **L4b**

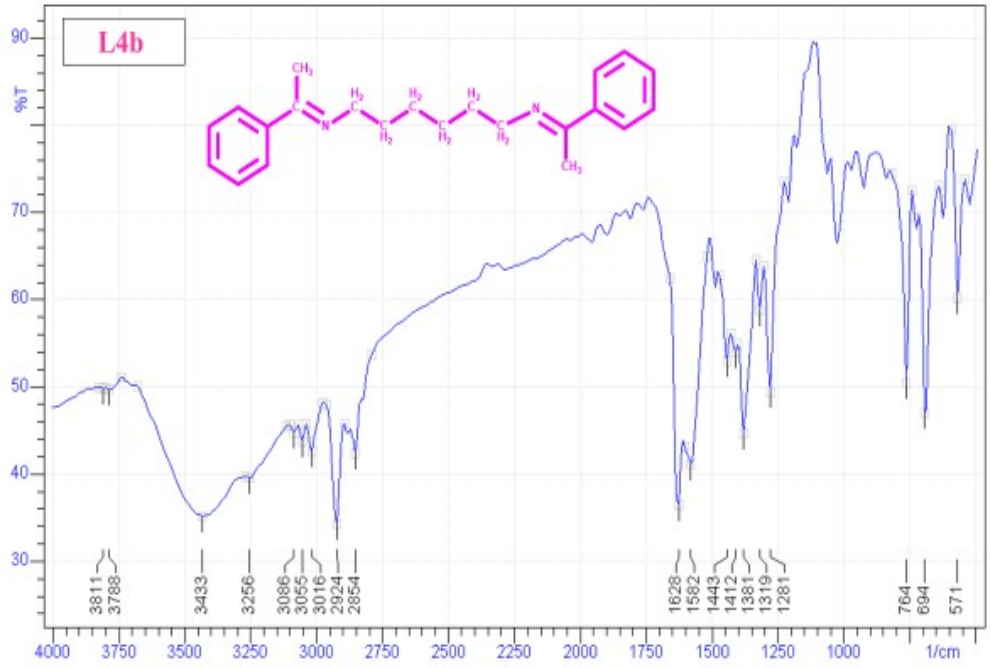

IR (cm^{-1} KBr pellet): 3811(w), 3433(m), 3256(w), 3055(w), 2924(m), 2854(w), 1628(vs), 1582(w), 1443(w), 1412(m), 1381(m), 1281(w), 794(m), 694(s),571(w).

Figure S23: ^{1}H NMR of **L4b**

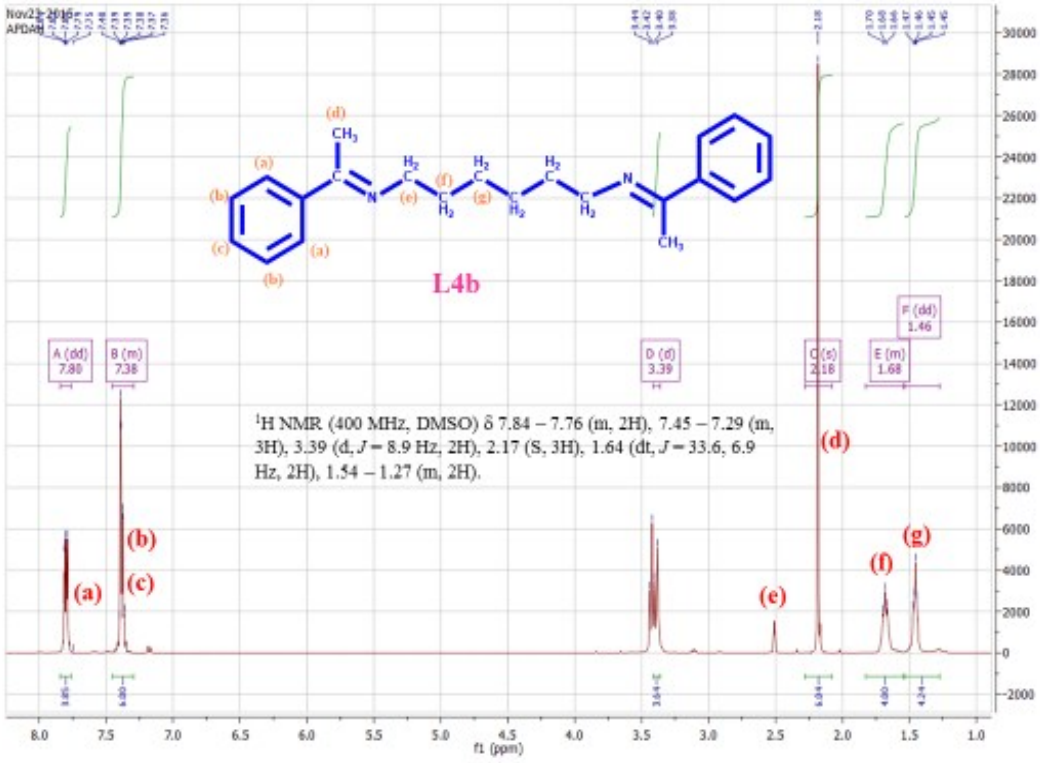

Figure S24: ^{13}C NMR of **L4b**

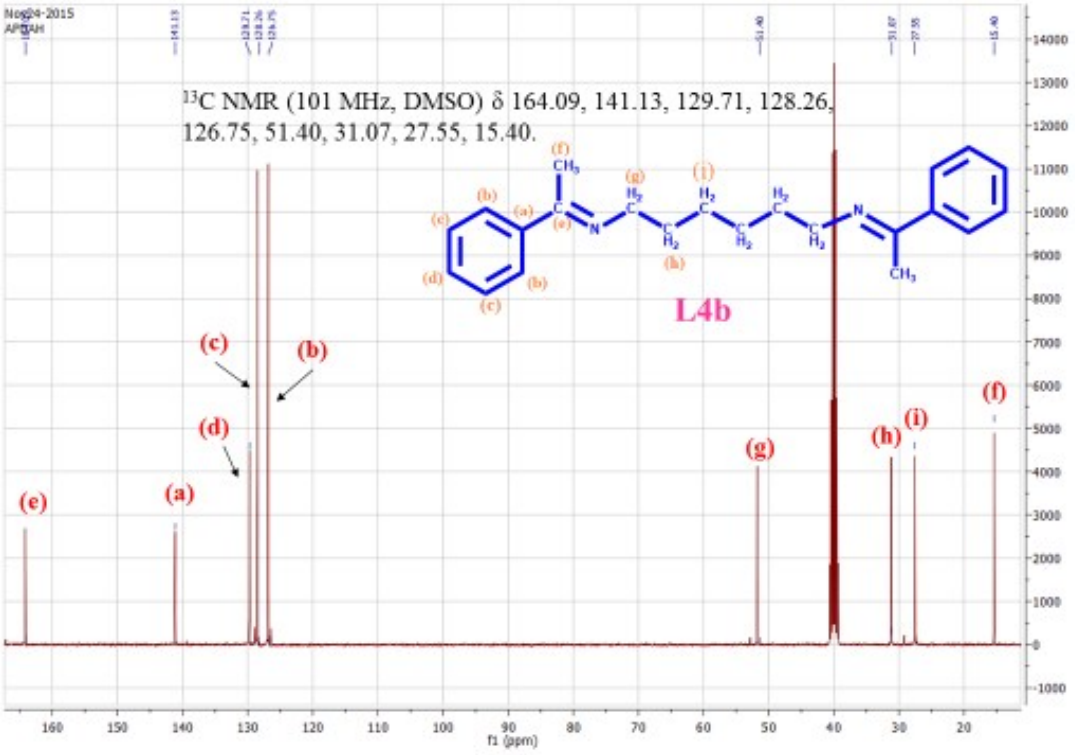

Figure S25: Experimental Powder XRD of **L2a**

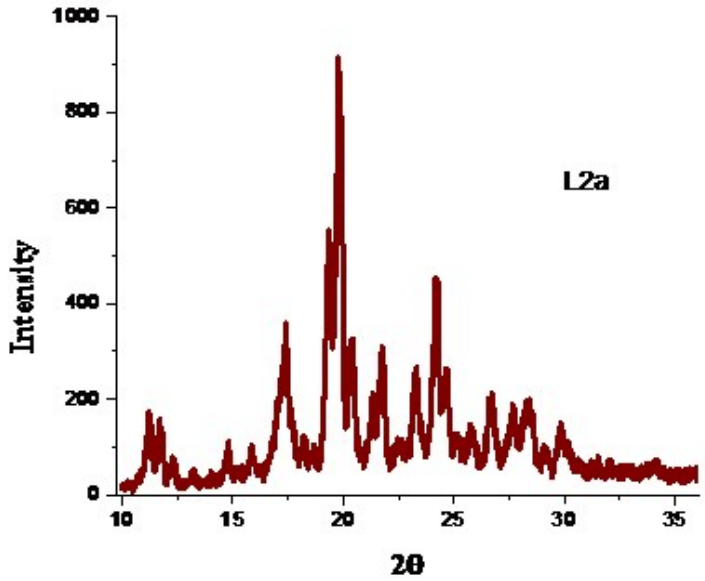

Figure S26: Experimental Powder XRD of **L3a**

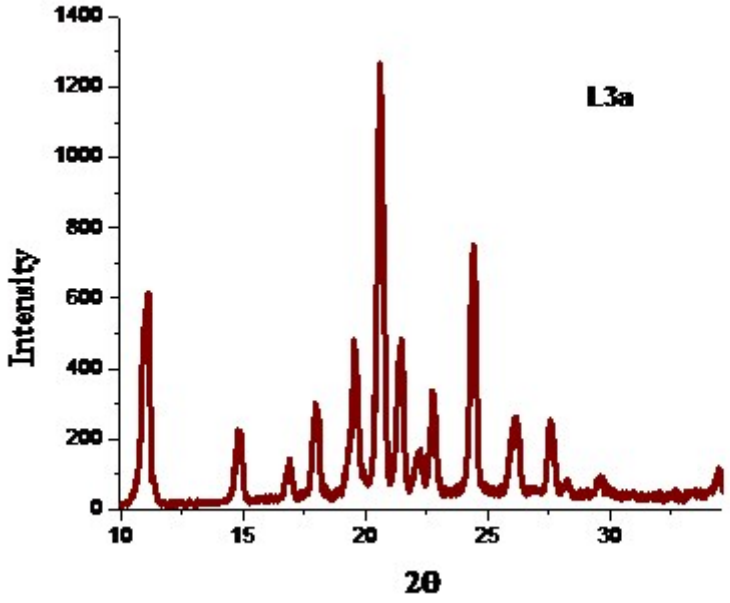

Figure S27: Experimental Powder XRD of **L3b**

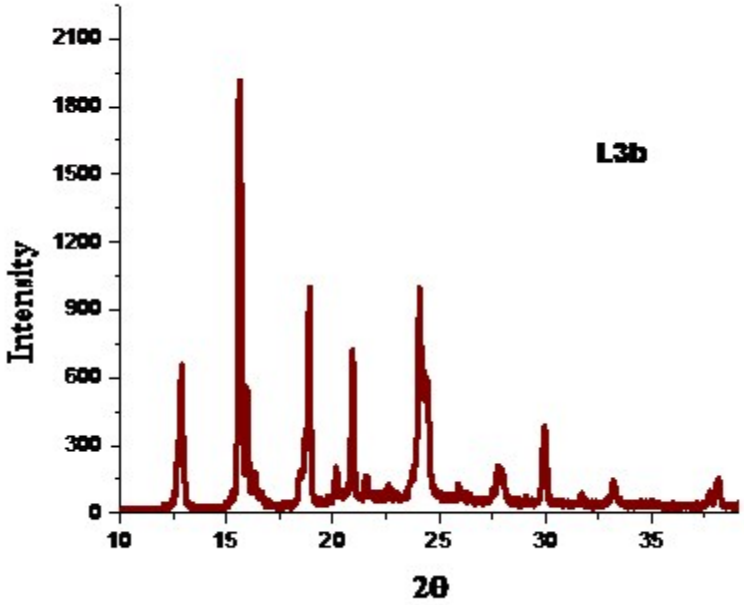

Figure S28: Experimental Powder XRD of **L4a**

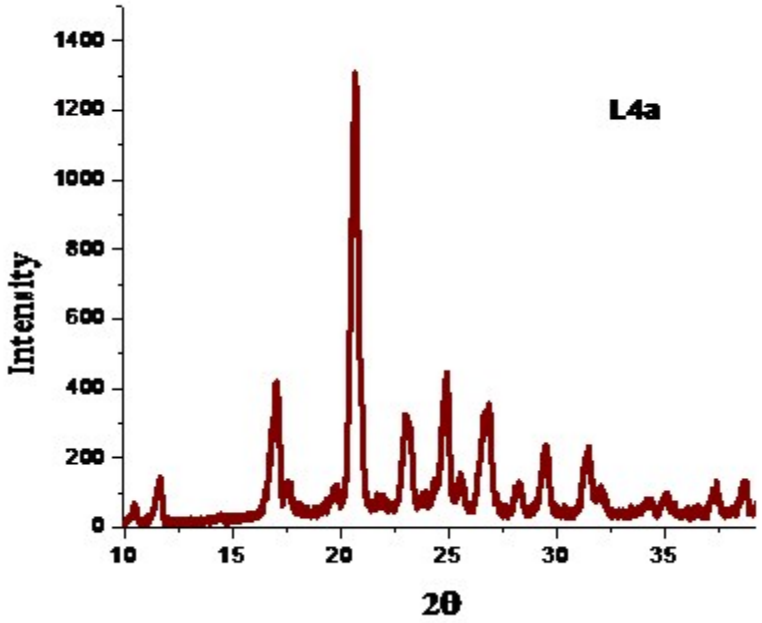

Figure S29: Experimental Powder XRD of **L4b**

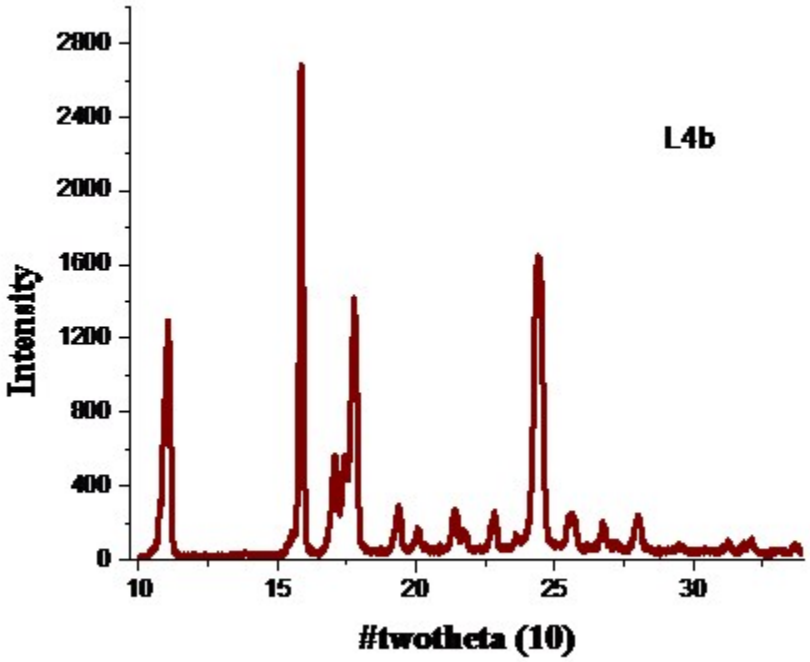

Figure S30: UV-Visible Spectrum of **L1a** in MeOH: Concentration : 10^{-4}M

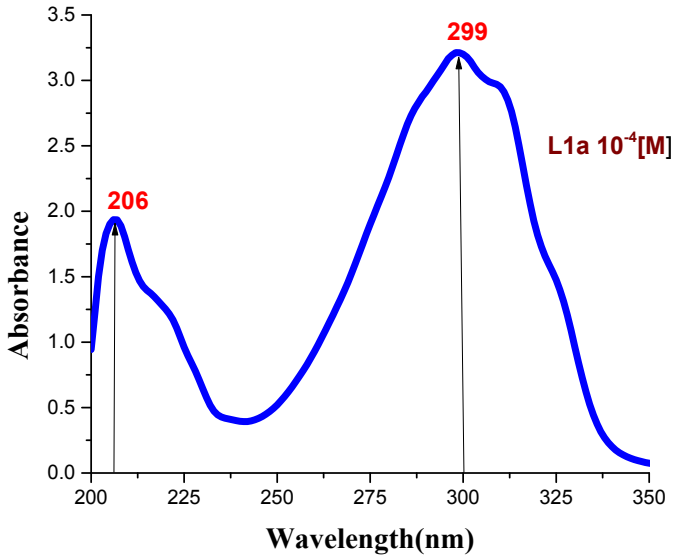

Figure S31: UV-Visible Spectrum of **L1b** in MeOH: Concentration: 10^{-4}M

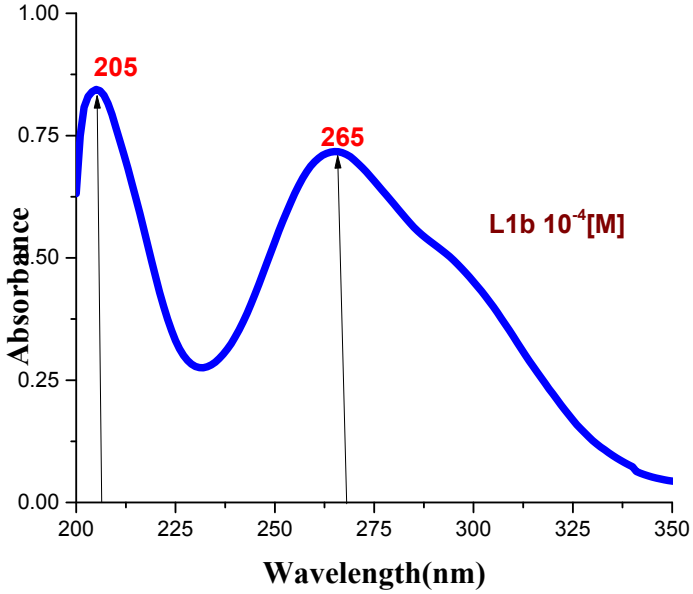

Figure S32: UV-Visible Spectrum of **L2a** in MeOH Concentration: 10^{-4}M

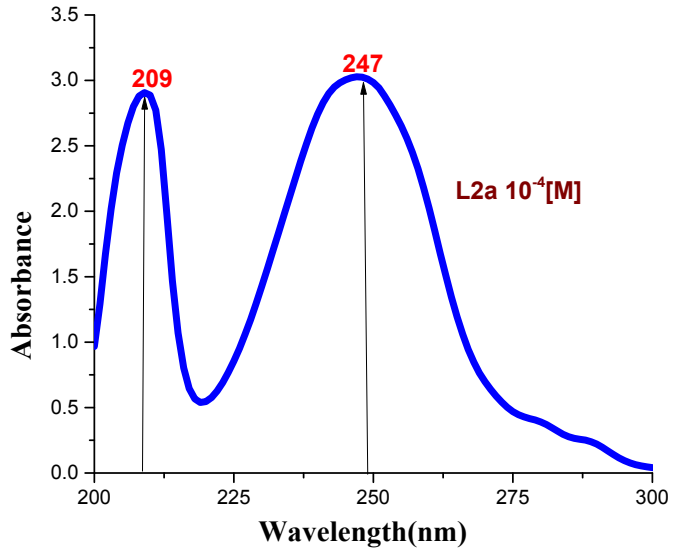

Figure S33: UV-Visible Spectrum of **L2b** in MeOH Concentration: 10^{-4}M

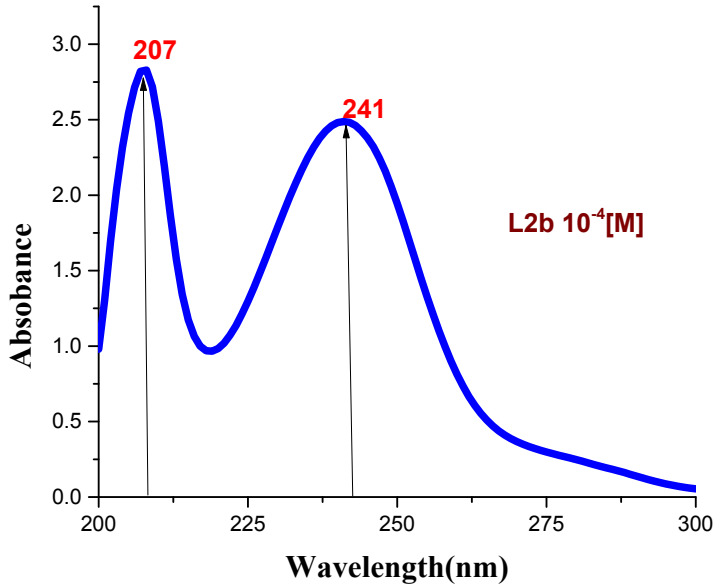

Figure S34: UV-Visible Spectrum of **L3a** in MeOH Concentration: 10^{-4}M

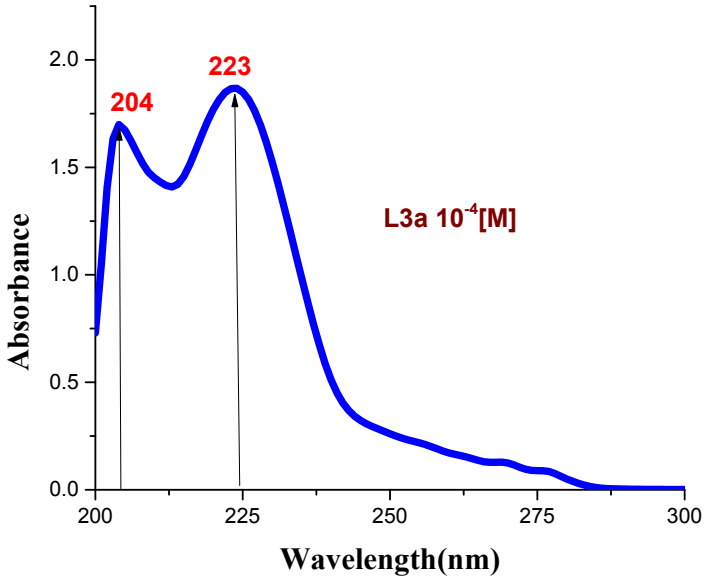

Figure S35: UV-Visible Spectrum of **L3b** in MeOH Concentration: 10^{-4}M

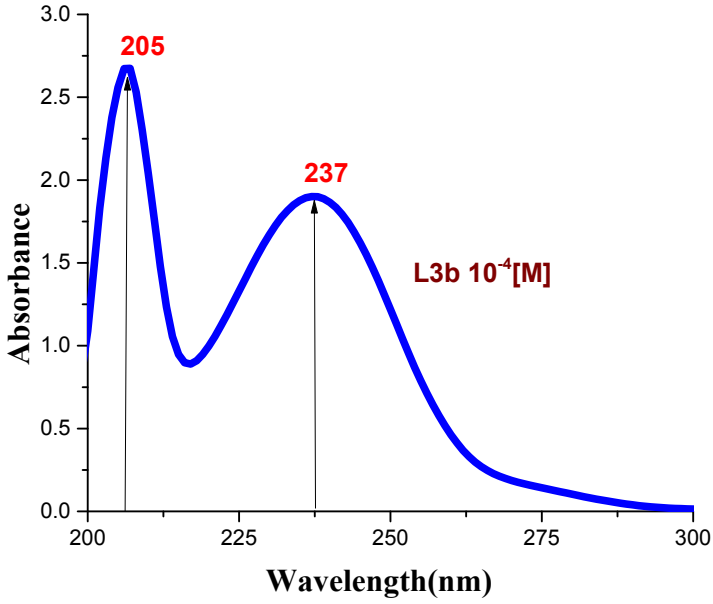

Figure S36: UV-Visible Spectrum of **L4a** in MeOH Concentration: 10^{-4}M

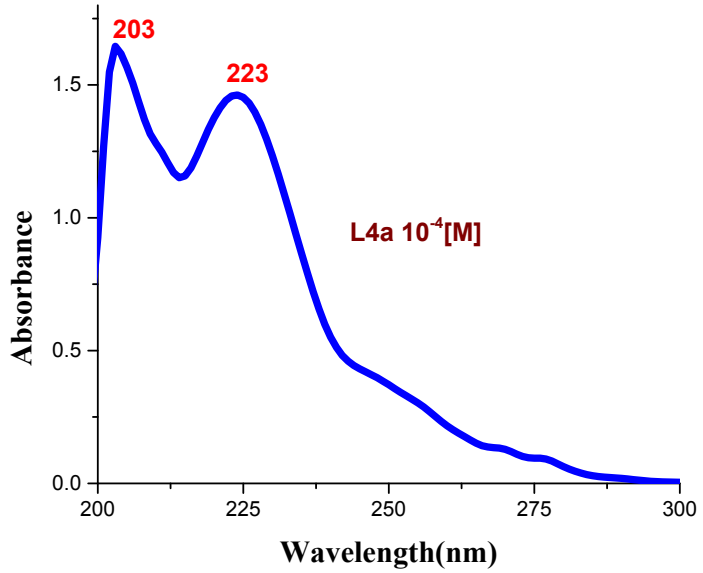

Figure S37: UV-Visible Spectrum of **L4b** in MeOH Concentration: 10^{-4}M

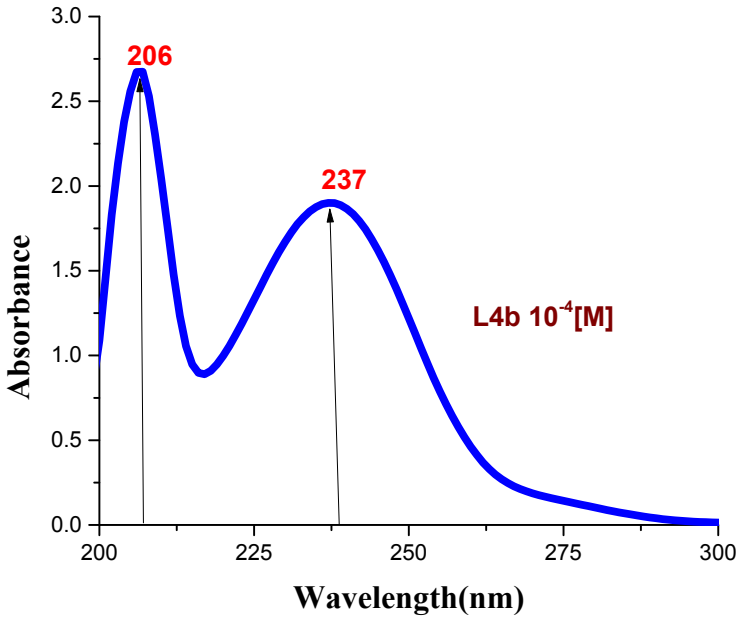

Figure S38: PL spectra of (a) **L3a** at an excitation wavelength of 420 nm; (b) **L3b** at excitation wavelength of 320 nm and 420 nm

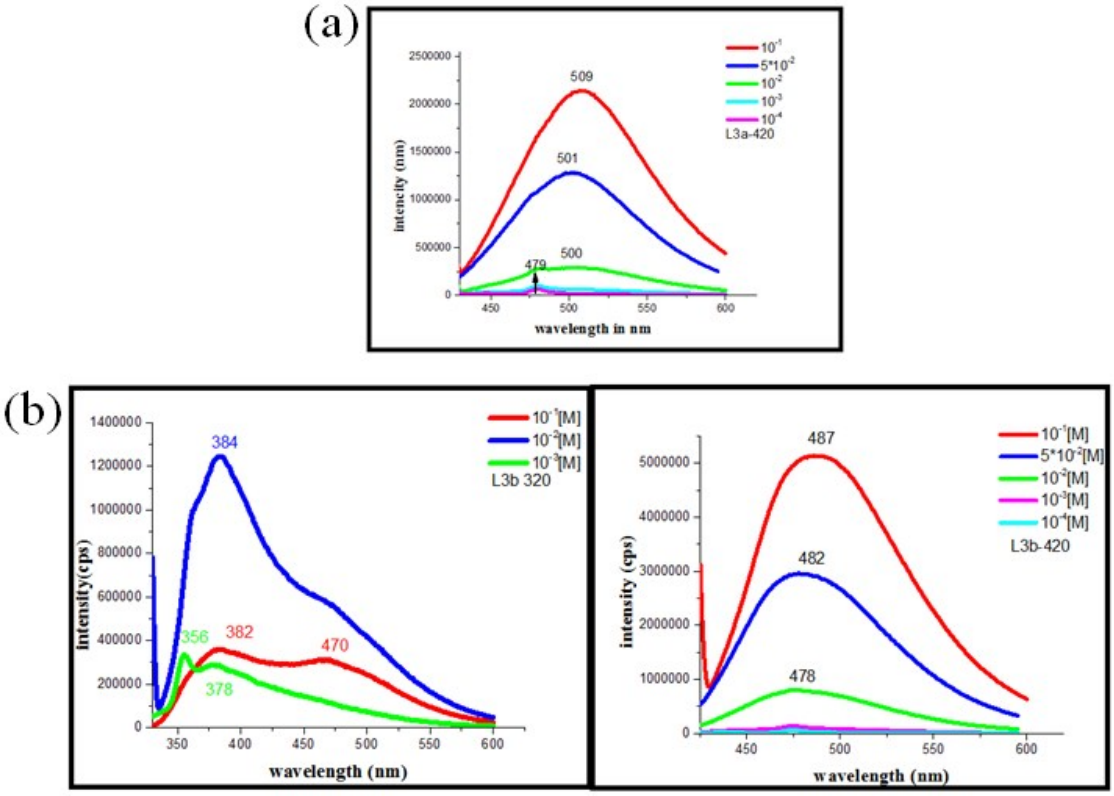

Figure 39: PL Spectra of (a) **L4a** in different concentrations at an excitation wavelength of 280nm; (b) **L4a** in different concentrations at an excitation wavelength of 450nm; (c) **L4b** in different concentrations at an excitation wavelength of 320nm; (d) **L4b** in different concentrations at an excitation wavelength of 420nm

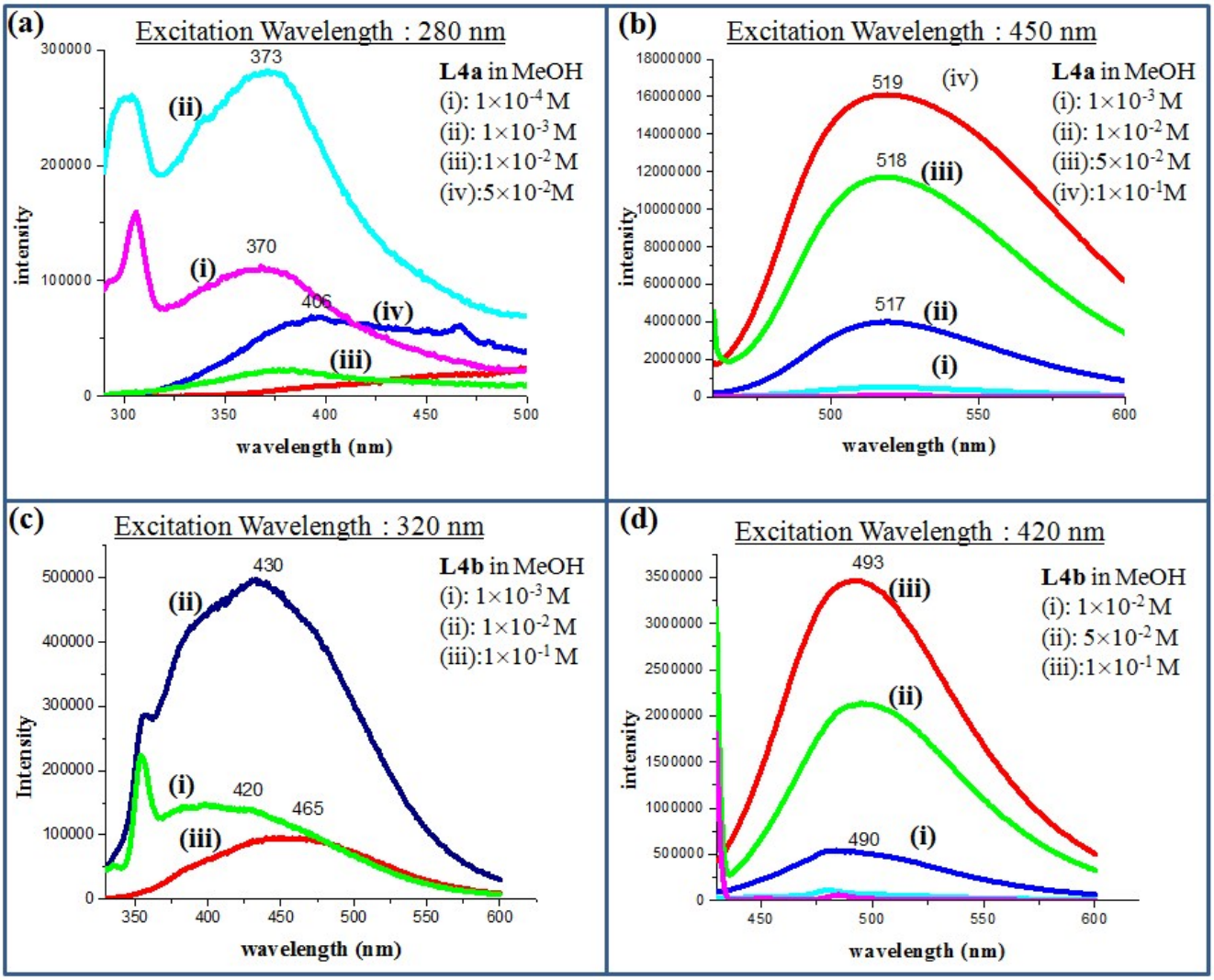

Figure S40: PL spectra of **L2a** and **L2b** in Solid State

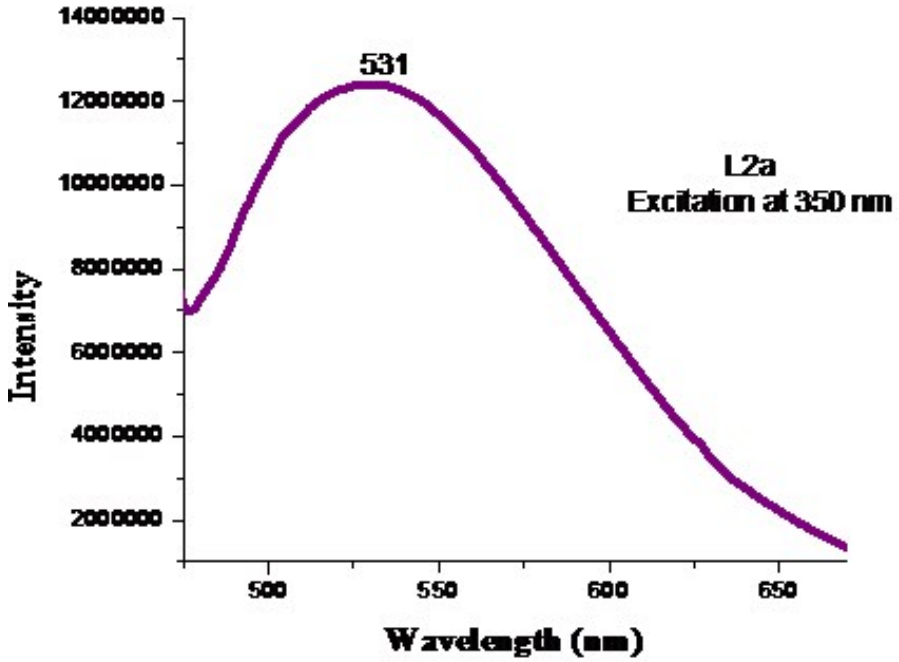

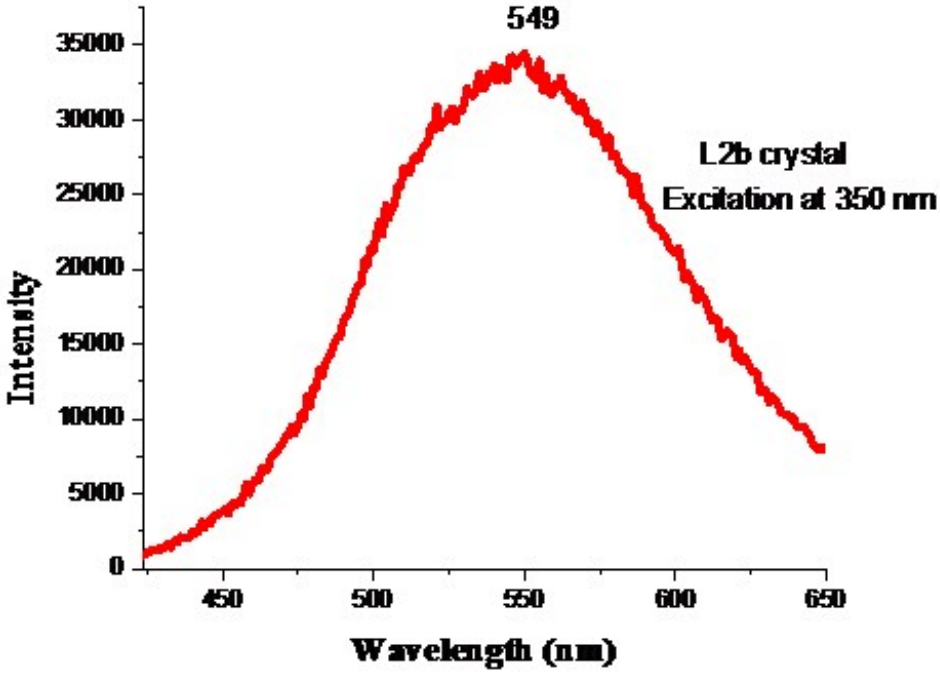

Figure S41: PL spectra of **L3a** in Solid State

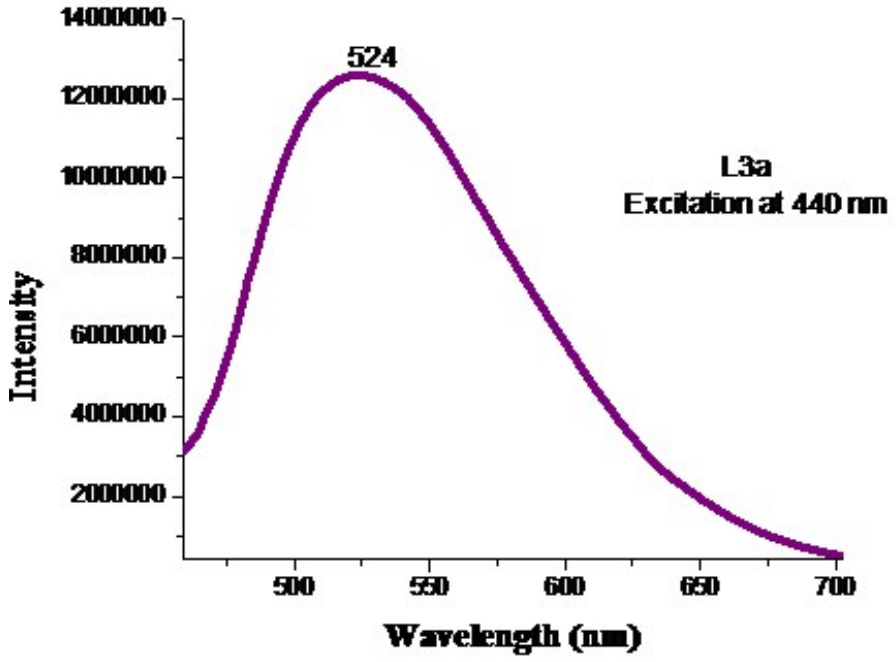

Figure S42: PL spectra of **L3b** in Solid State

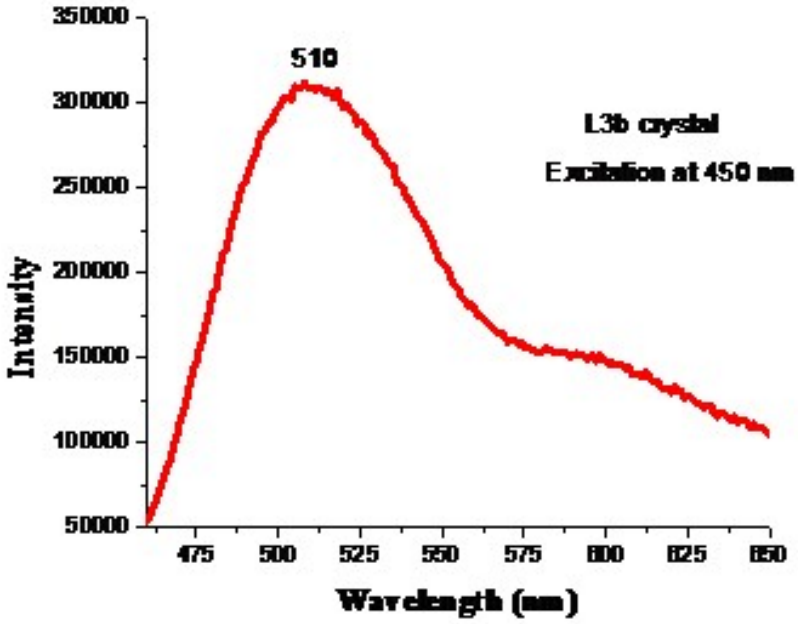

Figure S43: PL spectra of **L4a** in Solid State

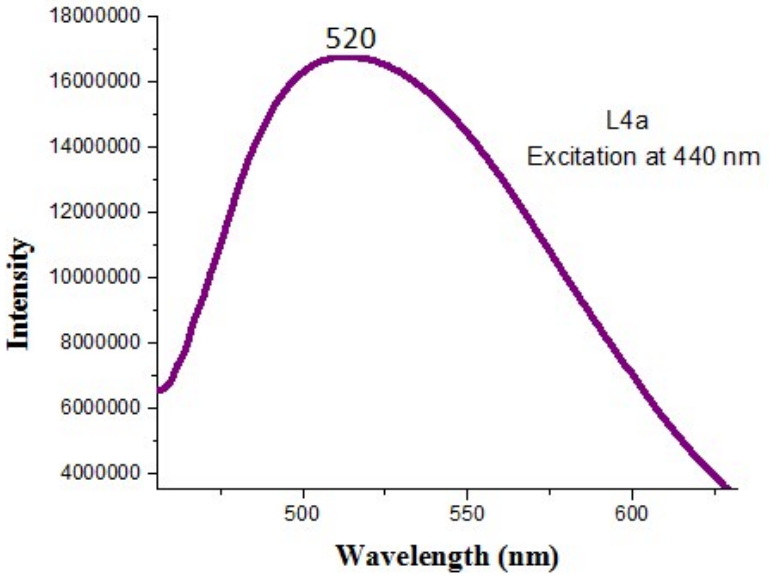

Figure S44: PL spectra of **L4b** in Solid State

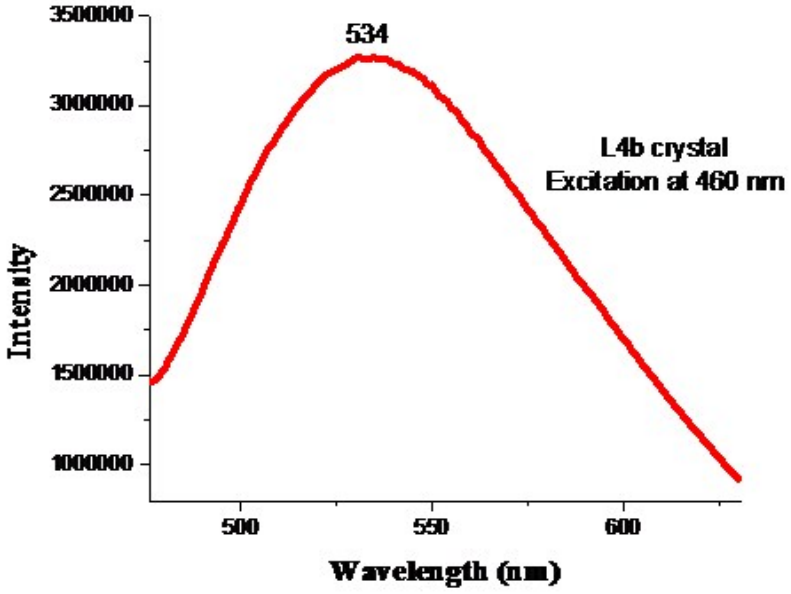

Table S1: $\lambda_{max.}$ in the PL Spectra in solutions of different concentration and at different excitations

λ_{ex}	300 nm		350 nm		400 nm		450 nm	
	Conc. (M)	λ_{em} (nm)	Conc. (M)	λ_{em} (nm)	Conc. (M)	λ_{em} (nm)	Conc. (M)	λ_{em} (nm)
L2a	0.1	439	0.1	435	0.1	474	0.1	518
	0.01	358,428	0.01	432	0.01	466	0.01	517
	0.001	359,426	0.001	431	0.001	453	0.001	517
	0.0001	330,364	0.0001	391,429	0.0001	452	0.0001	518
L2b	0.1	464	0.1	440	0.1	466	0.1	500
	0.01	365,431	0.01	435	0.01	459	0.01	490
	0.001	359,424	0.001	433	0.001	454	0.001	489
	0.0001	330,364	0.0001	391,429	0.0001	453	0.0001	489
λ_{ex}	320 nm		380 nm		420 nm		430 nm	
L3a	0.1	463	0.1	463	0.1	509	0.1	511
	0.05	459	0.05	461	0.05	501	0.05	504
	0.01	391,449	0.01	428,458	0.01	500	0.01	497
	0.001	353,386	0.001	428,460	0.001	479	0.0001	493
λ_{ex}	320 nm		350 nm		400 nm		450 nm	
L3b	0.1	382,470	0.1	469	0.1	477	0.1	508
	0.01	384	0.05	466	0.05	475	0.05	504
	0.001	356,378	0.01	392,463	0.01	473	0.01	503
			0.001	391,454	0.0001	453		
			0.0001	390,430				

λ_{ex}	280 nm		320 nm		380 nm		450 nm	
L4a	0.1	514	0.1	394	0.1	464	0.1	519
	0.05	406	0.05	386	0.05	462	0.05	518
	0.01	383	0.01	383	0.01	460	0.01	517
	0.001	304,373	0.001	380	0.001	460	0.001	517
	0.0001	306,370					0.0001	517
λ_{ex}	320 nm		380 nm		400 nm		420 nm	
	Conc. (M)	λ_{em} (nm)	Conc. (M)	λ_{em} (nm)	Conc. (M)	λ_{em} (nm)	Conc. (M)	λ_{em} (nm)
L4b	0.1	465	0.1	469	0.1	481	0.1	493
	0.01	356,430	0.05	468	0.05	479	0.05	493
	0.001	353,420	0.01	464	0.01	474	0.01	490
			0.001	429,461	0.001	453	0.001	480
			0.0001	428	0.0001	453	0.0001	484

Figure S45: Absorption and emission spectra (excitation 300nm) of the compounds

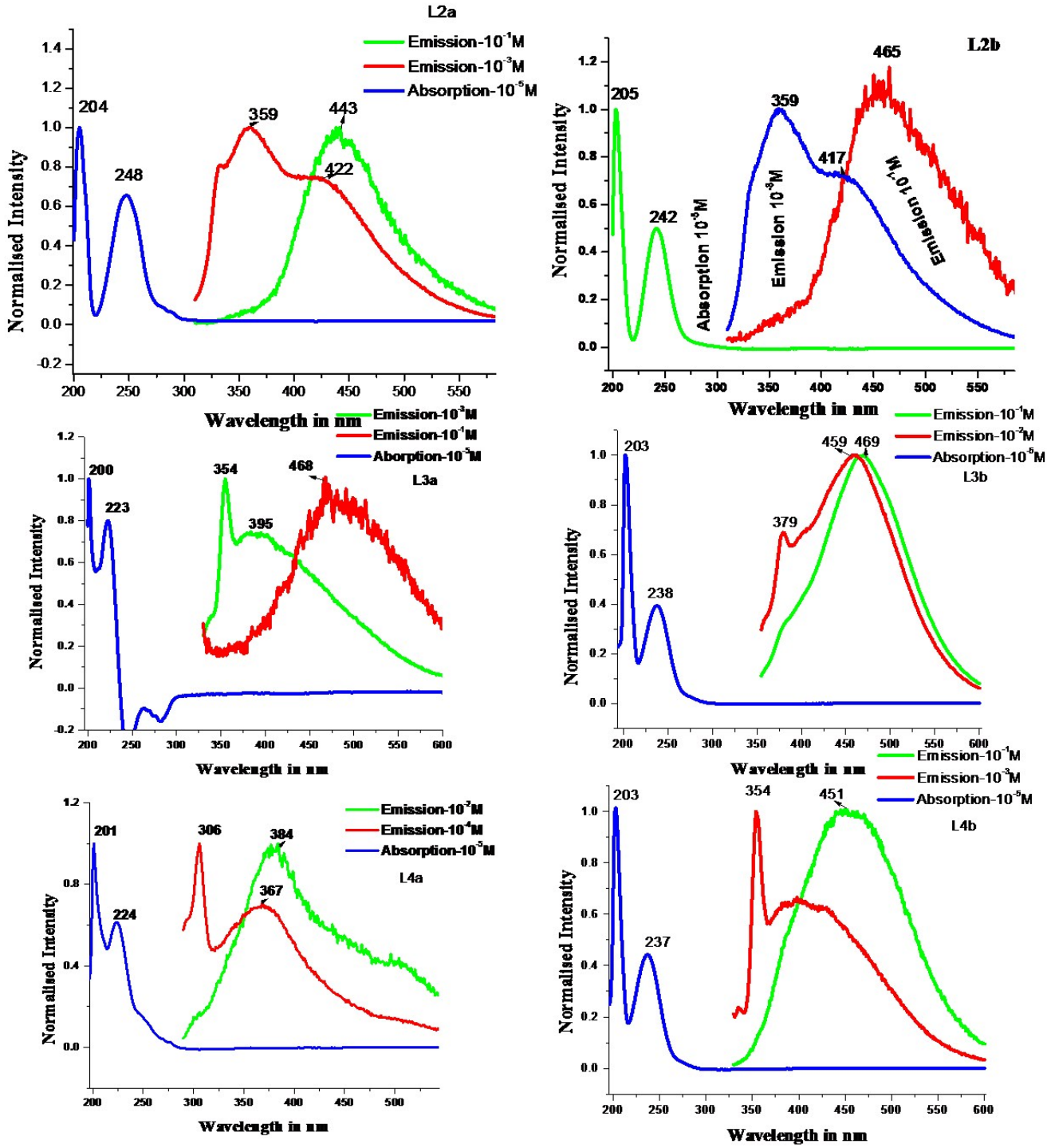

Table S2: Molar Extinction Coefficient of UV-Vis spectra of **L2b**, **L3a**, **L3b**, **L4a** and **L4b** in wavelengths near 300nm

Compounds		Molar Extinction coefficient (ϵ) ($M^{-1}cm^{-1}$)	Wavelength in nm
L2b	10^{-4}M	521 607 2796	349 330 284
	10^{-5}M	930 23170 45310	330 241 202
L3a	10^{-3}M	126.7	299
	10^{-4}M	259 375 1760 1338	345 300 269 277
	10^{-5}M	-136570 10250 12600	345 223 201
L3b	10^{-4}M	693 2255	349 275
	10^{-5}M	1620 20370 48380	349 238 202
L4a	10^{-4}M	493 1361 1842	347 277 269
	10^{-5}M	540 16720 26650	349 223 201
L4b	10^{-4}M	774 2365	348 278
	10^{-5}M	1710 29620 64060	348 237 202

Figure S46: TCSPC decay profiles of **L2a** in different concentration in MeOH with excitation at 375 nm

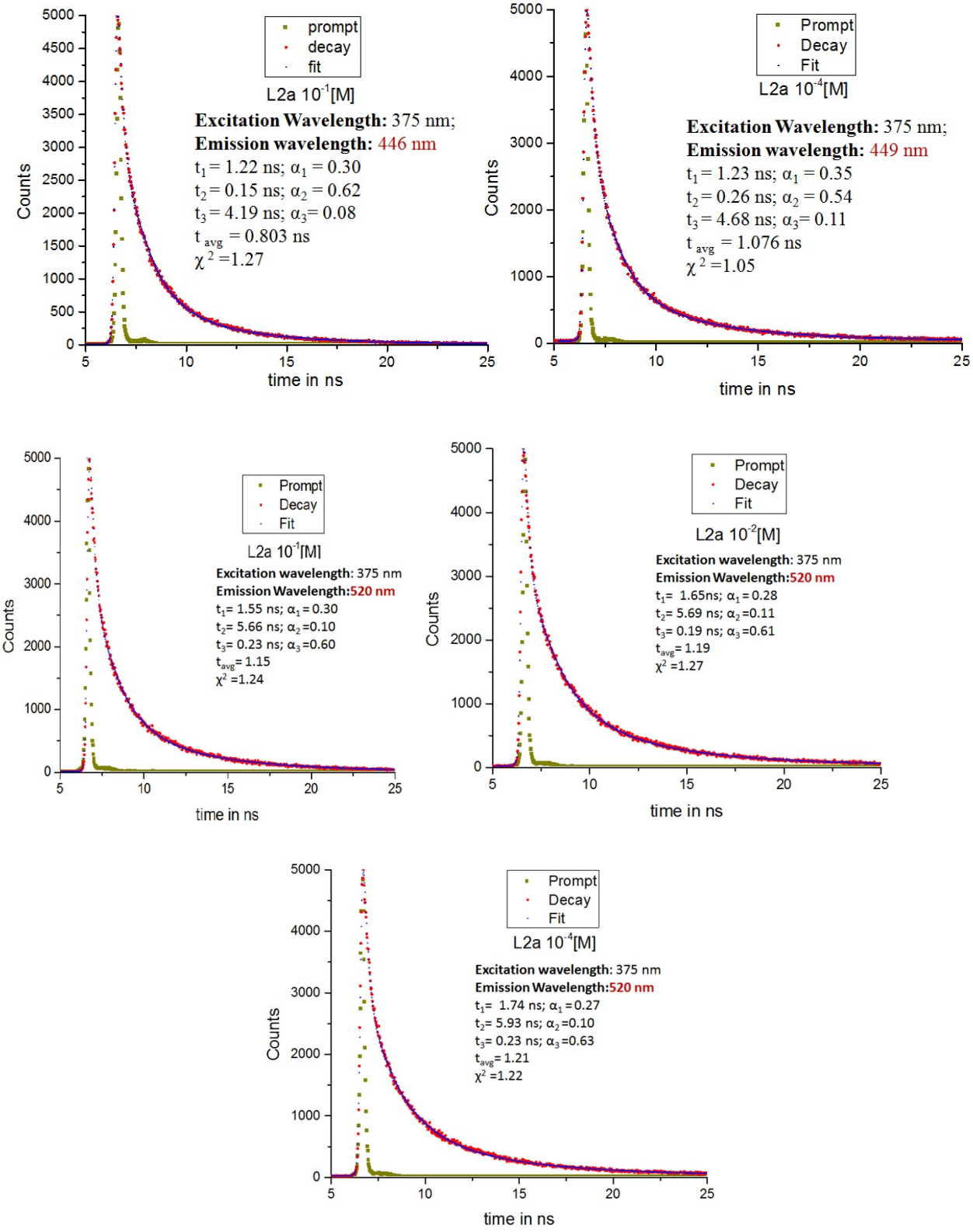

Figure S47: TCSPC decay profiles of **L2b** in different concentration in MeOH with excitation at 375 nm

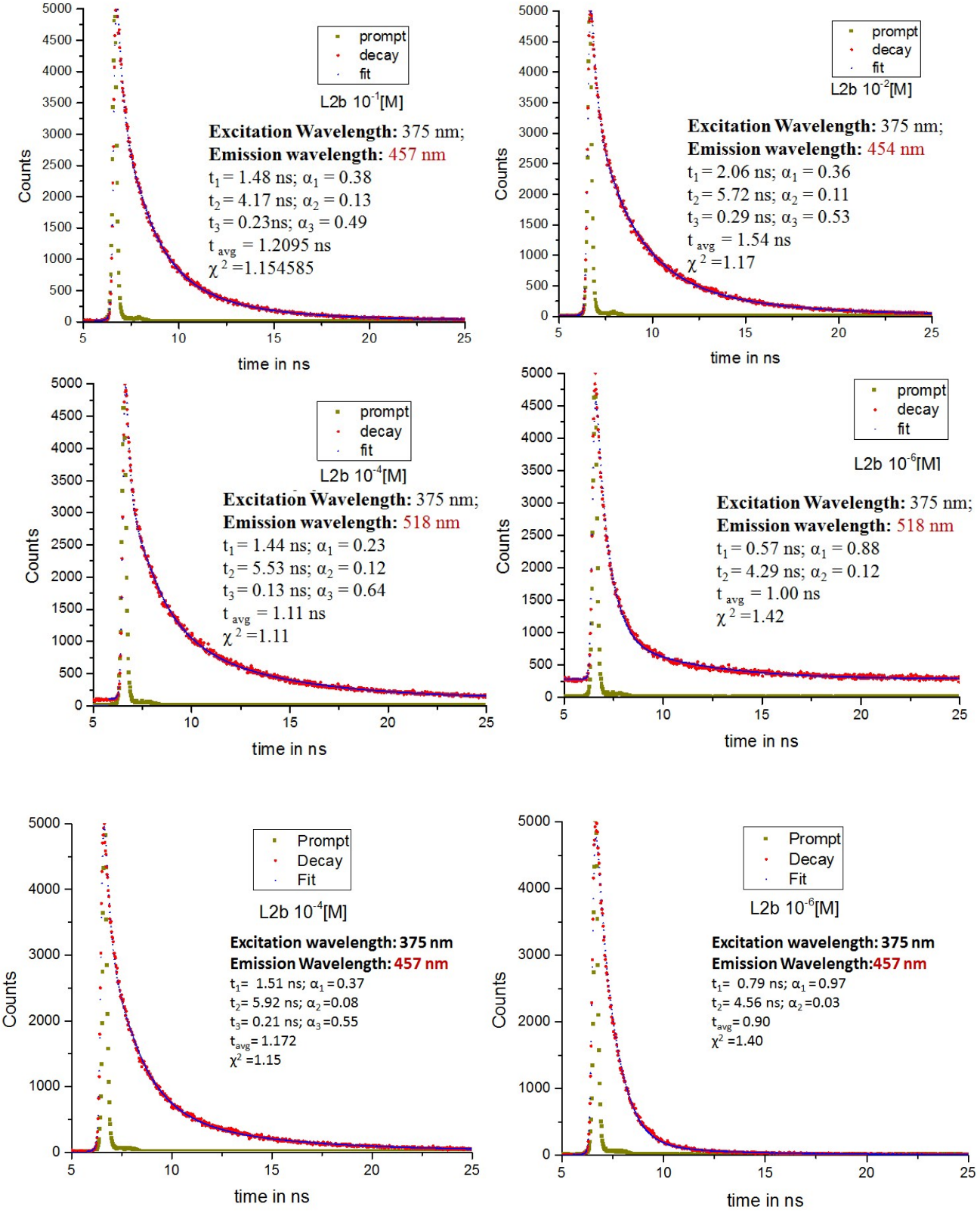

Figure S48: TCSPC decay profiles of **L3a** in different concentration in MeOH with excitation at 375 nm

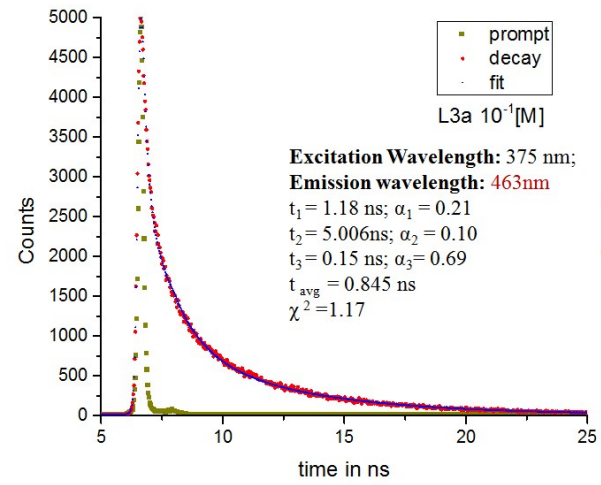

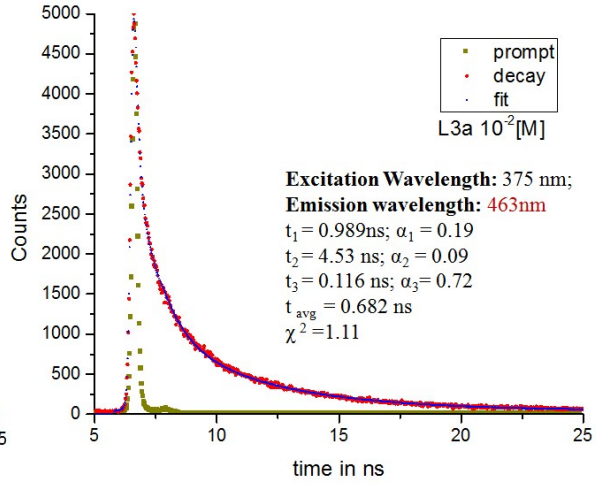

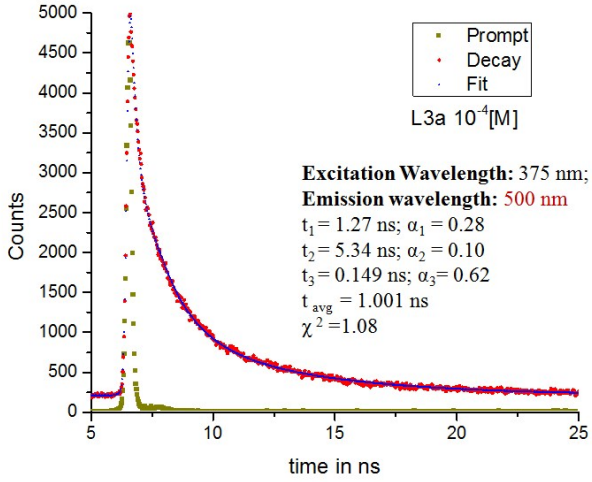

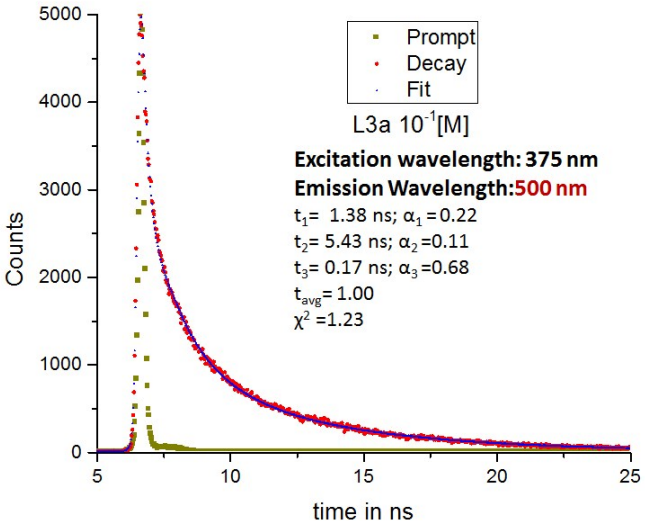

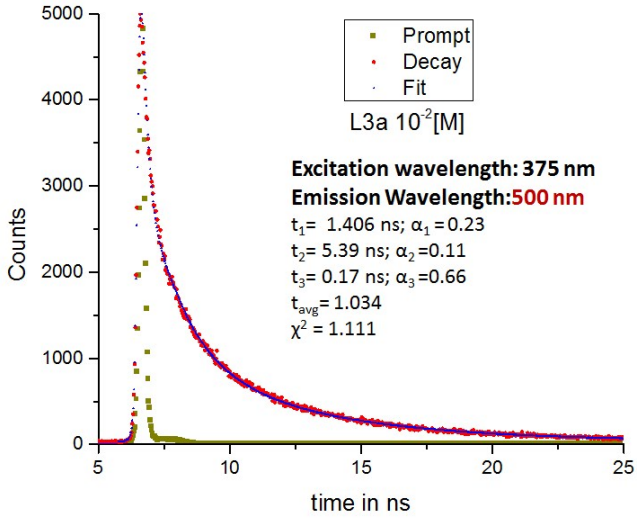

Figure S49: TCSPC decay profiles of **L3b** in different concentration in MeOH with excitation at 375 nm

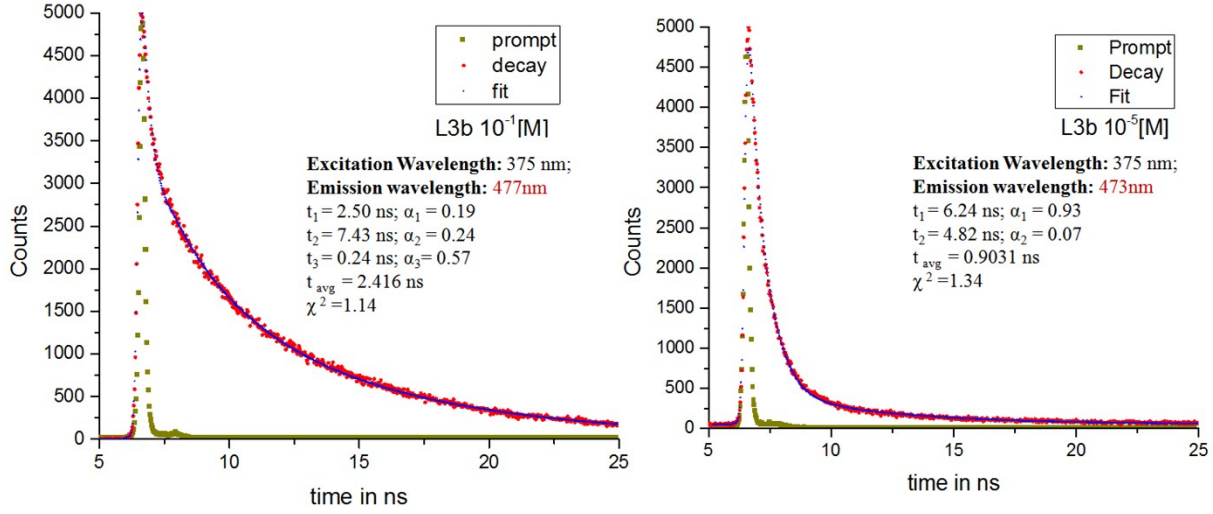

Figure S50: TCSPC decay profiles of **L4a** in different concentration in MeOH with excitation at 375 nm

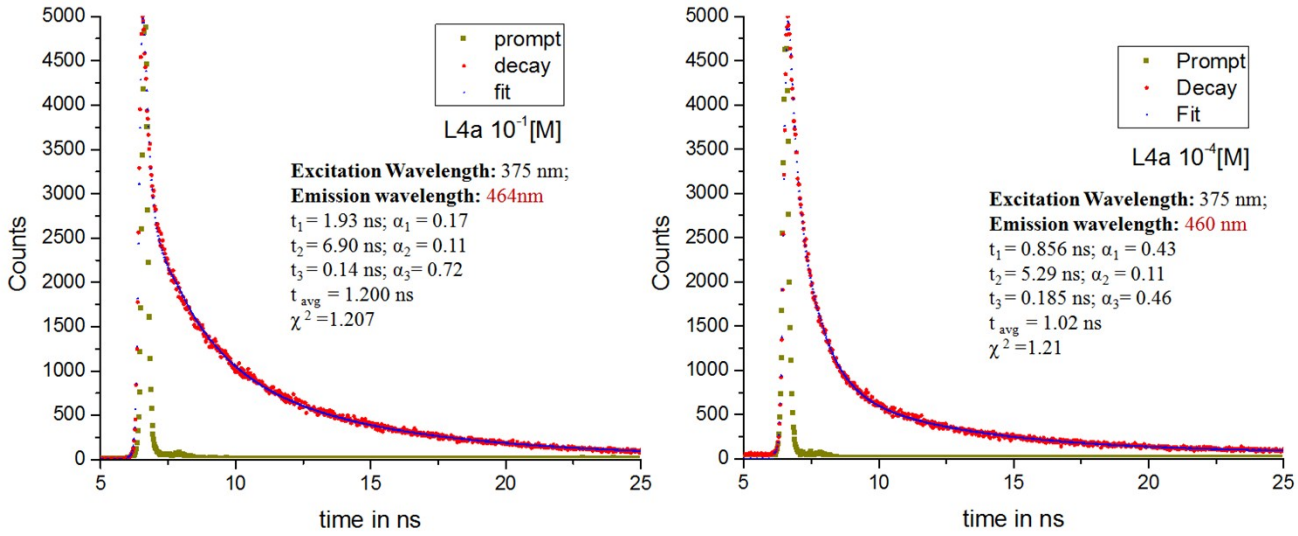

Figure S51: TCSPC decay profiles of **L4b** in different concentration in MeOH with excitation at 375

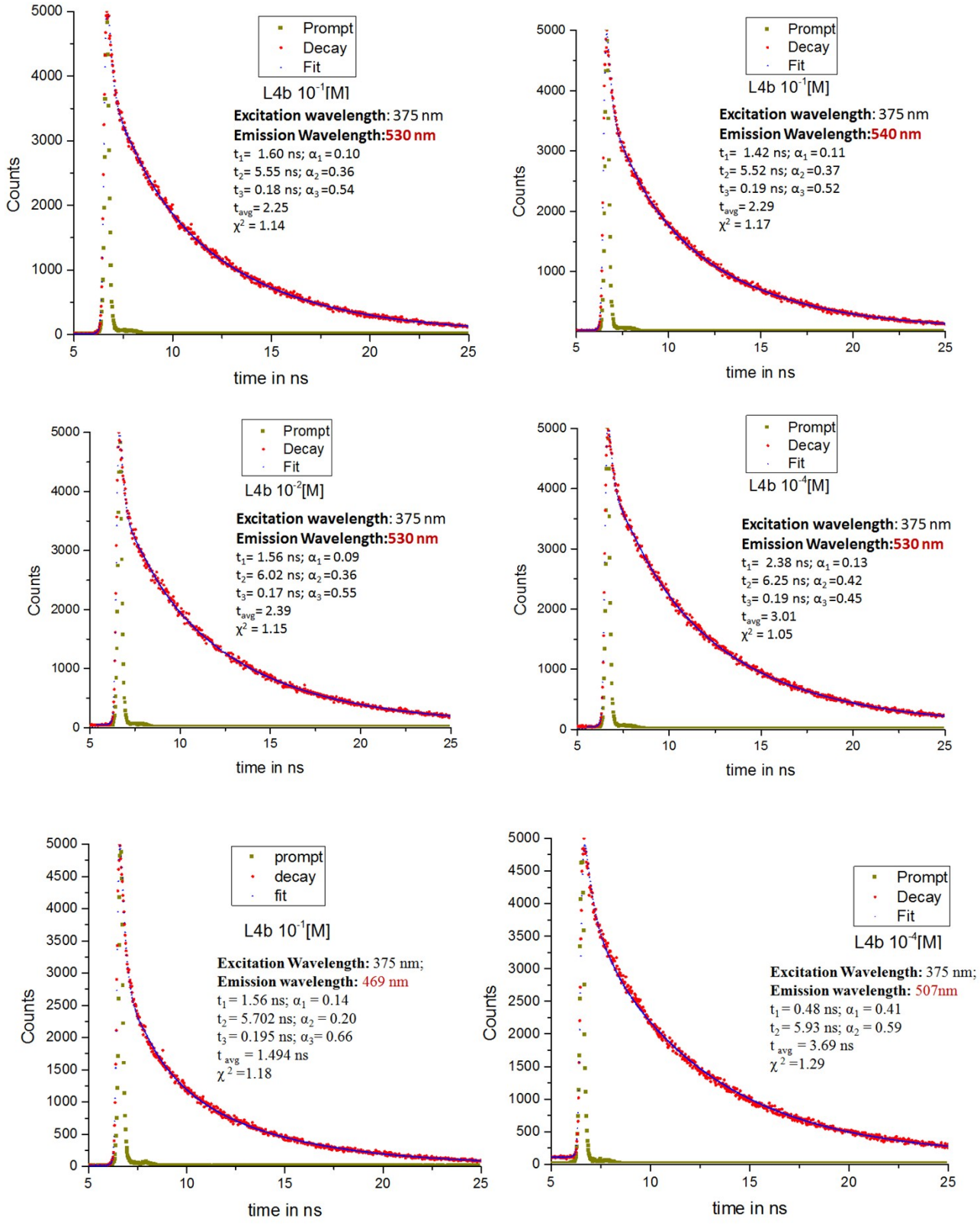

Table S3: Fluorescence lifetime data for **L2a**, **L2b**, **L3a**, **L3b**, **L4a** and **4b**

Excitation Wavelength = 375nm	τ_1 (ns)	τ_2 (ns)	τ_3 (ns)	τ_{avg} (ns)
L2a				
10^{-1} **M**; $\lambda_{Emission}$ 520nm	1.55 (α_1 0.30)	5.66 (α_2 0.10)	0.23 (α_3 0.60)	1.15 (χ^2 1.24)
10^{-1} **M**; $\lambda_{Emission}$ 446nm	1.22 (α_1 0.30)	0.15 (α_2 0.62)	4.19 (α_3 0.08)	0.803 (χ^2 1.27)
10^{-2}**M**; $\lambda_{Emission}$ 520nm	1.65 (α_1 0.28)	5.69 (α_2 0.11)	0.19 (α_3 0.61)	1.19 (χ^2 1.27)
10^{-4}**M**; $\lambda_{Emission}$520nm	1.74 (α_1 0.27)	5.93 (α_2 0.10)	0.23 (α_3 0.63)	1.21 (χ^2 1.22)
10^{-4}**M**; $\lambda_{Emission}$449nm	1.23 (α_1 0.35)	0.26 (α_2 0.54)	4.69 (α_3 0.11)	1.076 (χ^2 1.05)
L2b				
10^{-1}**M**; $\lambda_{Emission}$457nm	1.48 (α_1 0.38)	4.17 (α_2 0.13)	0.23 (α_3 0.49)	1.209 (χ^2 1.15)
10^{-2} **M**; $\lambda_{Emission}$454nm	2.06 (α_1 0.36)	5.72 (α_2 0.11)	0.29 (α_3 0.53)	1.540 (χ^2 1.17)
10^{-4} **M**; $\lambda_{Emission}$518nm	1.45 (α_1 0.23)	5.53 (α_2 0.12)	0.13 (α_3 0.64)	1.110 (χ^2 1.11)
10^{-4} **M**; $\lambda_{Emission}$457nm	1.51 (α_1 0.37)	5.92 (α_2 0.08)	0.21 (α_3 0.55)	1.172 ($\chi^2$1.15)
10^{-6} **M**; $\lambda_{Emission}$518nm	0.57 (α_1 0.88)	4.29 (α_2 0.12)	----	1.001 (χ^2 1.42)
10^{-6} **M**; $\lambda_{Emission}$457nm	0.79 (α_1 0.97)	4.56 (α_2 0.03)	----	0.90 (χ^2 1.40)
10^{-6} **M**; $\lambda_{Emission}$457nm	0.33 (α_1 0.38)	0.95 (α_2 0.61)	5.87 (α_3 0.01)	0.79 (χ^2 1.15)
L3a				
10^{-1}**M**; $\lambda_{Emission}$500nm	1.38 (α_1 0.22)	5.43 (α_2 0.11)	0.17 (α_3 0.68)	1.00 (χ^2 1.23)
10^{-1}**M**; $\lambda_{Emission}$463nm	1.19 (α_1 0.21)	5.01 (α_2 0.10)	0.15 (α_3 0.69)	0.845 (χ^2 1.17)
10^{-2}**M**; $\lambda_{Emission}$500nm	1.406 (α_1 0.23)	5.39 (α_2 0.11)	0.17 (α_3 0.66)	1.034 (χ^2 1.111)
10^{-2}**M**; $\lambda_{Emission}$463nm	0.99 (α_1 0.19)	4.53 (α_2 0.09)	0.12 (α_3 0.72)	0.682 (χ^2 1.11)
10^{-4}**M**; $\lambda_{Emission}$500nm	1.28 (α_1 0.28)	5.34 (α_2 0.10)	0.15 (α_3 0.62)	1.001 (χ^2 1.08)
L3b				
10^{-1}**M**; $\lambda_{Emission}$477nm	2.50 (α_1 0.19)	7.43 (α_2 0.24)	0.24 (α_3 0.57)	2.416 (χ^2 1.14)
10^{-5}**M**; $\lambda_{Emission}$473nm	6.24 (α_1 0.93)	4.83 (α_2 0.07)	----	0.903 (χ^2 1.34)
L4a				
10^{-1}**M**; $\lambda_{Emission}$464nm	1.93 (α_1 0.17)	6.90 (α_2 0.11)	0.15 (α_3 0.72)	1.201 (χ^2 1.20)
10^{-4}**M**; $\lambda_{Emission}$460nm	0.86 (α_1 0.43)	5.29 (α_2 0.11)	0.19 (α_3 0.46)	1.021 (χ^2 1.21)
L4b				
10^{-1}**M**; $\lambda_{Emission}$540nm	1.42 ($\alpha_1$0.11)	5.52 (α_2 0.37)	0.19 (α_3 0.52)	2.29 (χ^2 1.17)
10^{-1}**M**; $\lambda_{Emission}$469nm	1.57 (α_1 0.14)	5.70 (α_2 0.20)	0.19 (α_3 0.66)	1.495 (χ^2 1.18)
10^{-1}**M**; $\lambda_{Emission}$530nm	1.60 ($\alpha_1$0.10)	5.55 (α_2 0.36)	0.18 (α_3 0.54)	2.25 (χ^2 1.14)
10^{-2}**M**; $\lambda_{Emission}$530nm	1.56 (α_1 0.09)	6.02 (α_2 0.36)	0.17 (α_3 0.55)	2.39 (χ^2 1.15)
10^{-2}**M**; $\lambda_{Emission}$530nm	0.32 (α_1 0.53)	5.8 (α_2 0.47)	----	2.90 (χ^2 1.33)
10^{-4}**M**; $\lambda_{Emission}$530nm	2.38 (α_1 0.13)	6.25 (α_2 0.42)	0.19 (α_3 0.45)	3.01 (χ^2 1.05)
10^{-4}**M**; $\lambda_{Emission}$530nm	0.432 (α_1 0.41)	5.84 (α_2 0.59)	----	3.61 (χ^2 1.33)
10^{-4}**M**; $\lambda_{Emission}$507nm	0.49 (α_1 0.41)	5.94 (α_2 0.59)	----	3.692 (χ^2 1.29)

Figure S52: ^{1}H NMR spectra of **L2b** in $CDCl_3$ by changing the concentration of compound

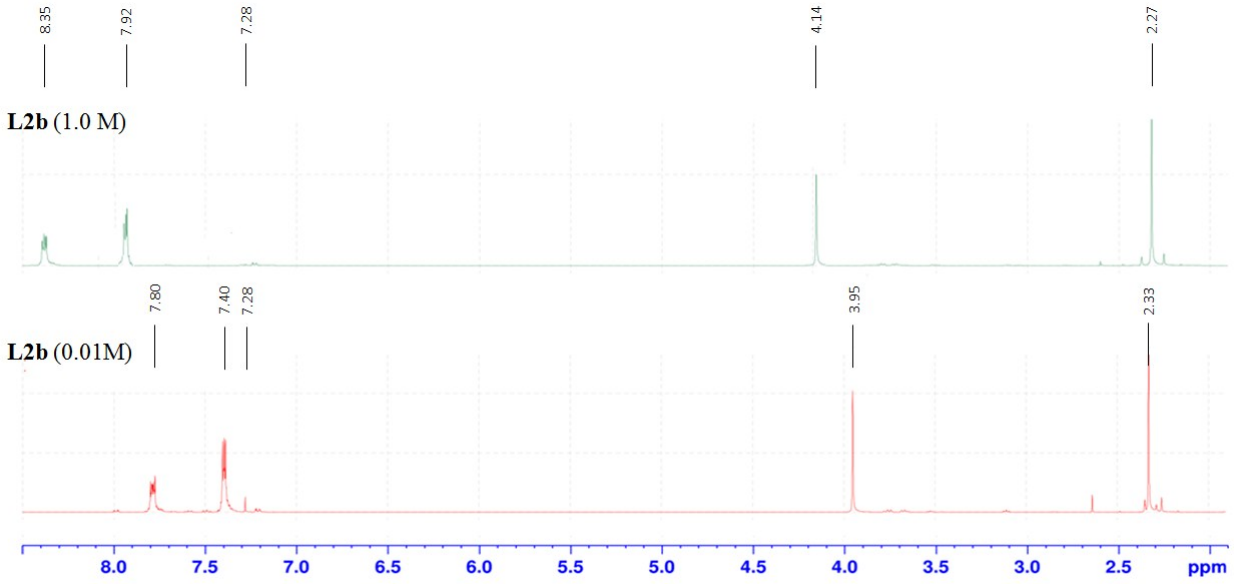

Figure S53: ^{1}H NMR spectra of **L2d** in $CDCl_3$ by changing the concentration of compound